

# Gravel-mantled megaripples of the Argentinean Puna: A model for their origin and growth with implications for Mars

S.L. de Silva<sup>1,†</sup>, M.G. Spagnuolo<sup>1</sup>, N.T. Bridges<sup>2</sup>, and J.R. Zimbelman<sup>3</sup>

<sup>1</sup>College of Earth, Ocean, and Atmospheric Sciences, Oregon State University, Corvallis, Oregon 97331, USA

<sup>2</sup>Johns Hopkins University Applied Physics Laboratory, Laurel, Maryland 20723, USA

<sup>3</sup>CEPS/NASM MRC 315, Smithsonian Institution, Washington, District of Columbia 20013-7012, USA

<sup>4</sup>Universidad Nacional de Salta, Av Bolivia 5150, 4400 Salta, Argentina

## ABSTRACT

Gravel “megaripples” in the Puna of Argentina are the most extreme aeolian megaripples on Earth and are useful analogs for aeolian processes on Mars. Field observations, supplemented by experimental and numerical constraints on wind characteristics and aeolian transport, reveal their conditions of formation and growth to be an aeolian geomorphology “perfect storm.”

The bedforms are formed on a substrate of weakly indurated ignimbrite, aeolian deflation of which yields a bimodal lag of lithics and pumice clasts onto an undulating surface. Under normal wind conditions in this region, the lithics are organized into bedforms on local upslopes and “highs” through creep induced by the impact of saltating sand and pumice. The gravel bedforms grow through “shadowing” and trap sand and silt that is gradually kinetically sieved down to “lift” the gravel mantle upwards to form the megaripples. These observations connote that the largest features are not ripples in the sense of migrating bedforms, but rather nucleation sites of wind-transported sediment. Strong control by bedrock topography means that the largest bedform wavelengths are not a result of particle trajectories, and this complicates their comparison with other ripples and may require a new classification.

Of relevance to Mars, the Puna megaripples are morphologically and contextually similar to small ripple-like transverse aeolian ridges (TARs). Moreover, the Puna gravels have similar equivalent weight (*mg*) to those composing granule ripples at Meridiani Planum, and their local origin may have implications for the origin of sediment in martian

aeolian bedforms. Finally, the stable yet dynamic character of the Puna megaripples could help reconcile current models of TARs with periodic bedrock ridges that may be produced by aeolian erosion.

## INTRODUCTION

The predominance of aeolian (wind-driven) activity as a surface-modifying agent on Mars has been recognized throughout the history of telescopic, satellite, and robotic investigation of the planet. The most obvious expressions of aeolian processes are manifested in dunes (Breed and Grow, 1979; Greeley et al., 1992; Bridges et al., 2013), yardangs (wind-eroded landforms; Ward, 1979; Mandt et al., 2008, 2009), sand ripples (Sullivan et al., 2007; Silvestro et al., 2010), and transverse aeolian ridges (TARs) (Bourke et al., 2003; Wilson and Zimbelman, 2004). TAR is a non-genetic general term proposed for linear to curvilinear aeolian features. Since their first recognition, the origin of TARs has remained an area of healthy debate, with the central question being whether they are small dunes or large ripples. The answer to this question is critical to understanding the way that wind works on the martian surface, with implications for National Aeronautics and Space Administration (NASA) strategic interests in the area of human and robotic exploration of Mars. The challenge is that to answer the questions of origin, we need to understand the details of shape, size, and spatiotemporal development of the bedforms, and the size and density of the grains that form them. Although the resolution of remotely sensed data has improved rapidly, down to 25 cm/pixel with HiRISE (McEwen et al., 2007), we are still not capable of resolving sediment-size distributions from orbit (Zimbelman, 2008). Until we can do this, our understanding of aeolian processes on Mars will remain limited to the few lander and

rover sites. Thus, we rely heavily on our understanding of similar features on Earth as analogs both in terms of form and process. Recent rover investigations of martian TARs provide perhaps the most definitive data (e.g., Sullivan et al., 2005). These observations have revealed granule ripples similar to those on Earth. Studies have confirmed that granule ripples on Earth are potential analogs for ripple-like TARs on Mars (Zimbelman, 2010).

Coarse gravel bedforms in the Puna of Argentina represent some of the most extreme aeolian deposits on Earth in terms of particle properties and inferred formation conditions (Milana, 2009; de Silva et al., 2010, 2012). These gravel bedforms are built on a local substrate of ignimbrites and composed of a bimodal association of dense ( $>2 \text{ g cm}^{-3}$ ) lava and metamorphic clasts up to 2.5 cm in diameter and pumice clasts ( $<1.5 \text{ g cm}^{-3}$ ) up to 5 cm in diameter, making these the coarsest-grained aeolian bedforms yet described on Earth. While the mechanisms of origin and formation are debated (Milana, 2009; de Silva, 2010; Milana et al., 2010), it is clear that these bedforms represent extreme conditions that define an end member of the spectrum of terrestrial granule ripples. Indeed, Greeley and Iversen (1985) included granule ripples and other ripples variously termed “giant,” “erosion,” “sand ridges,” and “pebble ridges” in their *megaripples* class defined as having wavelengths up to 25 m. Based on characteristics described below we have determined that morphologically the Puna bedforms are ripples and not dunes, and due to their extreme morphology we follow Greeley and Iversen (1985) and describe them as megaripples. However, we note that the Puna features are *gravel mantled*, rather than being entirely composed of gravel as the terms gravel ripple or gravel megaripple may imply.

The Puna bedforms have several areas of relevance to Mars. The gravel bedforms are morpho-

<sup>†</sup>E-mail: desilvas@geo.oregonstate.edu

logically similar to small TARs and consist of materials that have similar equivalent weight ( $mg$ ) to those composing the granule ripples at Meridiani Planum, Mars. The pumice and lithics in the Puna are  $\sim 1/3$  the density of basalt and hematite making up the Meridiani granule ripples, respectively (Sullivan et al., 2005). However, the gravity on Mars is  $\sim 1/3$  that on Earth, so their relative equivalent weights are approximately analogous. Additionally, the spatial relationships among megaripples, topography, and bedrock in the Puna are analogous to relationships among TARs, topography, and bedrock on Mars. Finally, understanding the origin of the gravel may provide information on the source of aeolian sediments on Mars (e.g., Burr et al., 2012; de Silva et al., 2012).

We report here on the results of our study of the Puna gravel megaripples, present a model for their origin and growth, and explore the implications for Mars. In doing so, we will demonstrate that the largest features are not ripples in the sense of migrating bedforms, but rather nucleation sites of wind-transported sediment. This is an important distinction that has implications for their formation and classification.

## GEOLOGIC BACKGROUND

The gravel megaripples have developed in five distinct fields in close proximity to each other in the region of Catamarca, Argentina, loosely centered around  $26^{\circ}36'S$ ,  $67^{\circ}38'W$  (Fig. 1). Part of the Argentinean Puna, this region has base elevations above 3000 m in a region of high winds. Yardangs and more modern wind streaks on the Puna attest to strong northwesterly winds going back at least 2 m.y. and thus record large-scale atmospheric circulation patterns across the continent (Strecker et al., 2007). Wind records for the Puna are rare. Milana (2009) presented data from a mine located 300 km south at a comparable altitude to the gravel megaripple fields. These show that wind speeds of  $100 \text{ km h}^{-1}$  (63 mph) were quite common and at least eight wind gusts in a five-year period exceeded  $250 \text{ km h}^{-1}$  (156 mph) up to  $440 \text{ km h}^{-1}$  (275 mph)—a world record. We present here a recently acquired data set from two meteorological stations located at  $25^{\circ}06'S$ ,  $68^{\circ}20'W$  (altitude 5200 m), and at  $25^{\circ}03'S$ ,  $68^{\circ}13'W$  (altitude 4092 m),  $\sim 160 \text{ km NNE}$  and  $\sim 180 \text{ km NNE}$ , respectively, from the study area. These stations recorded wind velocity over a period of seven years. The data show large monthly ranges from a few kilometers per hour to rare gusts as high as  $240 \text{ km h}^{-1}$ . Monthly mean velocities are between  $35$  and  $50 \text{ km h}^{-1}$  (Fig. 2). These two data sets indicate

that the region is subject to very strong winds throughout the year. Any journey through this area would likely encounter saltating sand throughout the course of any given day.

The fields vary in extent from 50 to 600  $\text{km}^2$ , representing the largest areas of gravel ripples yet described. Each field is a separate “basin” demarcated by bounding volcanic and metamorphic “basement” highlands, while the main surface lithology in the basins is late Pleistocene pyroclastic deposits (mainly ignimbrite) ranging in age from 70,000 to 13,000 years (de Silva, 2010). These quartz-rich rhyolitic ignimbrites are weakly to moderately indurated and have been carved up by the wind to produce prominent yardangs and demoiselles (de Silva et al., 2010). They contain  $\sim 10\%$  by volume of exotic lithic clasts with densities ranging from  $2.6$  to  $3 \text{ g cm}^{-3}$ , and up to 20% crystal-poor pumice clasts with densities of  $\sim 0.8\text{--}1.3 \text{ g cm}^{-3}$ . Both lithics and pumice are locally enriched due to local flow and depositional characteristics. Erosion liberates these clasts and the crystals from the matrix ash, which is quickly elutriated away leaving a lag of crystals (dominated by quartz), andesite-rich lithics, and pumice fragments. The profile of yardangs shows a pronounced erosional reentrant with a maximum between 1.5 and 2 m above the base providing a proxy for the saltation profile. The dominant instrument of erosion is saltating quartz crystals derived from the ignimbrites themselves (de Silva et al., 2010).

Each field is distinct in lithological characteristics and macroscopic appearance, reflecting different mixtures of lithic clasts that make up the gravels. Locally derived pumice is the other main constituent of the gravels (Fig. 3).

The largest of the fields is the Campo Piedra Pomez (CPP) field that covers an area of  $\sim 600 \text{ km}^2$  in an approximately NNE-SSW-trending rectangle centered around  $26^{\circ}36'17.30''S$ ,  $67^{\circ}34'50.46''W$ . Elevation ranges from  $\sim 3800 \text{ m}$  in the south on the northern flank of the Pliocene to recent La Hoyada volcanic complex that houses the 70 ka Cerro Blanco caldera, to 3000 m in the north just to the south of Carachi Pampa cinder cone. The gravel field is built on bedrock of the 70 ka Campo Piedra Pomez ignimbrite and associated plinian fall deposits from the Cerro Blanco caldera complex (Arnosio et al., 2005). Here, dark megaripples prevail, reflecting the dominance of dark lava and older ignimbrite fragments.

Other significant fields are to the west of the basement ridge that defines the western boundary of the CPP. The largest of these extends to the east of Laguna Purulla (LP), covering an area of  $127 \text{ km}^2$  centered on  $26^{\circ}39'49.97''S$ ,  $67^{\circ}48'55.83''W$ . Elevation ranges from 3700 m

in the west on the margin of Laguna Purulla, to 4100 m in the east on the flanks of La Hoyada. The LP field is dominated by dark gravels that reflect the dominance of andesitic lava and vitrophyre fragments.

Immediately to the north from the LP field is the Campo Purulla (CP), located adjacent and downslope of the Cerro Purulla volcano to the west. This small field covers an area of  $\sim 12 \text{ km}^2$  centered on  $26^{\circ}37'12.27''S$ ,  $67^{\circ}46'00.66''W$ , at an elevation of  $\sim 3850 \text{ m}$  to 3950 m. Although it is broadly contiguous with the LP field, it is distinct in albedo, reflecting the distinct source of the gravels in this sub-basin. Red-brown clasts of the immediate basement-forming Upper Miocene Rosada ignimbrite and light quartz-rich fragments of Paleozoic basement are found in abundance along with the ubiquitous andesite clasts. The basement is overlain by the 13 ka Purulla ignimbrite that forms the immediate substrate to the gravel bedforms of interest.

Another distinct sub-basin to the north of CP is the Salar de Incahuasi (SI) field, so called because of its location on the southern shores of the narrow N-S-extending playa of the same name. It covers an area of  $54 \text{ km}^2$  centered around  $26^{\circ}31'53.61''S$ ,  $67^{\circ}41'36.93''W$ . Like CP, the basement clasts from the Rosada ignimbrite and older metamorphic basement are mixed with the andesite clasts, giving the gravels a brownish hue that is distinct from the darker gravels dominated by andesite in the CPP and LP fields. The gravel bedforms are built on the eroded surface of the 70 ka Campo Piedra Pomez ignimbrite, in this case the western ramp of this pyroclastic unit that was emplaced on the Rosada ignimbrite and older basement (Arnosio et al., 2005; Ortiz, 2011).

The smallest and most distinct field is the “White Barchan” field, so called because of its proximity to spectacular barchan dunes to the east of the CPP. This field covers only  $0.1 \text{ km}^2$  centered around  $26^{\circ}35'57.44''S$ ,  $67^{\circ}26'46.27''W$ , at  $\sim 3030 \text{ m}$ . It is highlighted because of the dominance of basement milky quartz clasts in the gravels, unique among the Puna megaripples. These are the smallest and least coarse gravel ripples. They will not be discussed further in this paper.

We focus here on the observations that illuminate the origin and growth of the gravel bedforms. It is striking that the coarse gravel bedforms in all the fields are formed where the immediate substrate is weakly to moderately indurated rhyolitic ignimbrites. In particular, gravel bedforms appear to be temporally and spatially related to prominent yardangs and demoiselles in the ignimbrites (de Silva, 2010). Moreover, the association of coarse, low-density pumice with dense clasts in these bedforms is

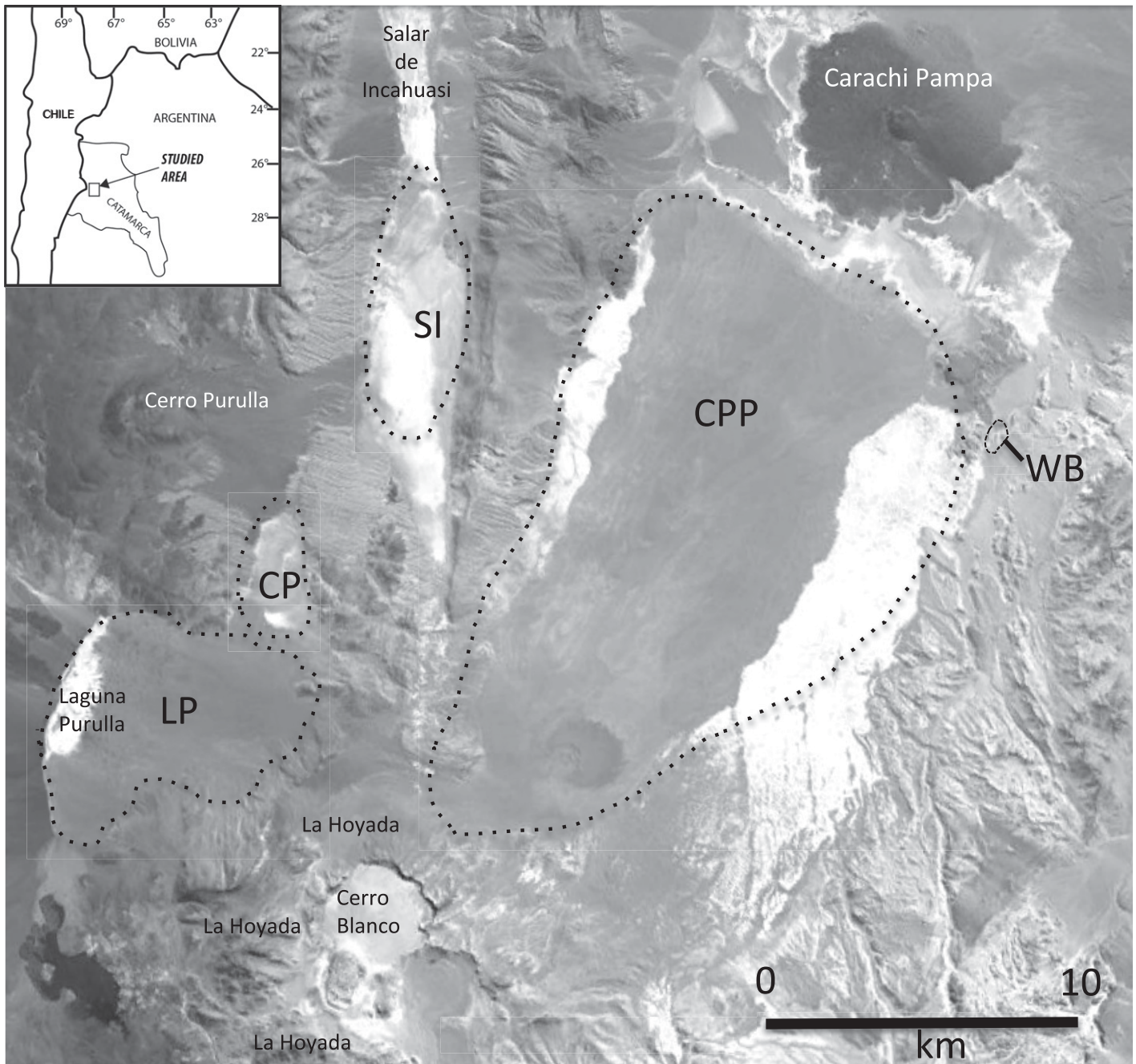


**Figure 1.** Location and areal footprint of the gravel megaripple fields in the Puna of Argentina. CPP—Campo Piedra Pomez; LP—Laguna Purulla field; CP—Campo Purulla field; SI—Salar de Incahuasi field; WB—White Barchan field. Base image was extracted from Google Earth. Inset map shows regional context of the field area.

also obvious. These three first-order observations suggest a strong relationship between the erosion of the ignimbrites and the development of the gravels and subsequent bedforms. We find that the most instructive relationships are found where relations between yardangs, gravels, and ignimbrite substrate are most clearly seen in the eastern edge of the CPP field, and those in the SI and CP fields.

## METHODS AND RESULTS

### Field Observations

Where well developed, the gravel bedform surfaces consist of a bimodal association of dense ( $>2.5 \text{ g cm}^{-3}$ ) volcanic and metamorphic clasts and lighter, both in albedo and density ( $<1.5 \text{ g cm}^{-3}$ ), pumice clasts up to 5 cm diam-

eter. Typically the pumice clasts are  $\sim 2.5\times$  the size of the gravel clasts they are spatially associated with in a gravel bedform. In the more mature areas, pumice is rare and small. The best-developed bedforms cap topography with amplitudes as high as 2 m and wavelengths of 30 m or more (Fig. 3C). Profiles of the bedforms made using a profiling technique referenced to a laser and string line above the features, along

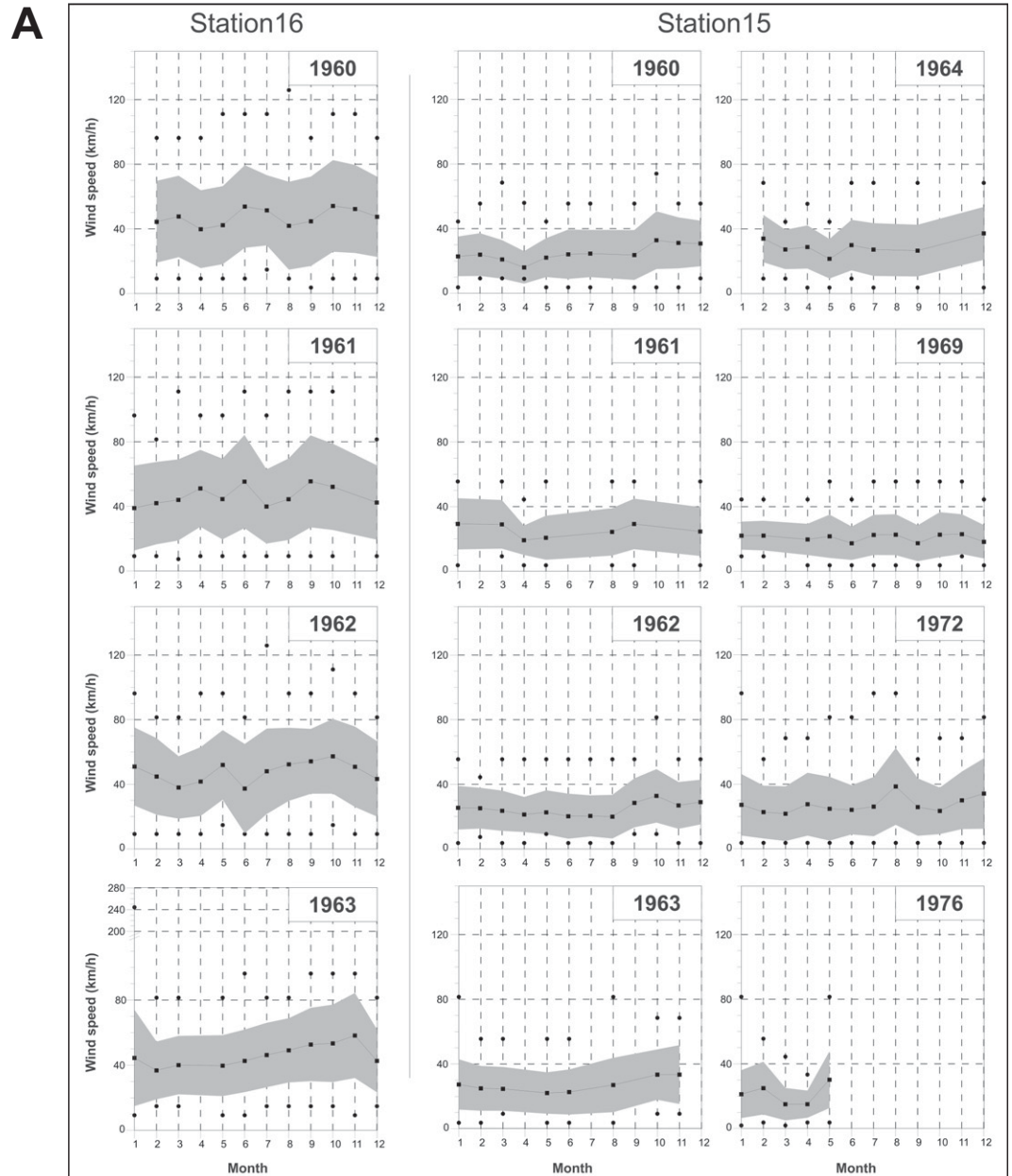


**Figure 2** (on this and following page). (A) Monthly mean wind velocities (squares), standard deviation (gray area), and maximum and minimum values (circles), for different years, recorded by two Argentinean Meteorological Service weather stations. Station 16 was located at 25°06'S, 68°20'W, altitude 5200 m; station 15 was located at 25°03'S, 68°13'W, altitude 4092 m. Data were obtained from the Banco de Datos of the Department of Atmosphere and Ocean Sciences, Facultad de Ciencias Exactas y Naturales (FCEN), Universidad de Buenos Aires (UBA) (<http://www-atmo.at.fcen.uba.ar/bancomedatos.php>).

with Brunton measurements, show significant variability among sites. Megaripples in the CP and SI show more symmetry between lee and stoss slopes than do those in the CPP and LP (Fig. 4A). Despite differences between sites, most of the measurements show that Puna features plot together in the megairipple cluster from Zimelman et al. (2012), but show a distinctive shift to larger width for the same aspect ratio of other megairipples, representing what seems like an end-member group between different-grain-size megairipples (Fig. 4B). Most interestingly, in size and aspect the Puna megairipples are morphologically and contextually similar to the small-scale TARs, which might be more related

to ripple-type structures than the larger TARs (Shockey and Zimelman, 2013).

Trenching into the bedforms reveals that the largest gravel bedforms make up ~30 cm of the 2 m amplitude of the topography (Fig. 5). The upper 10 cm of the bedform is dominated by crudely bedded coarse gravels, while the lower portion contains significantly more sandy and some silty material <125 mm (3  $\Phi$ ; Krumbein Phi scale [Krumbein and Aberdeen 1937]) and becomes progressively well sorted toward the core and base of the bedform. Rarely laminations and distinct internal sandy beds can be found. The coarsest particles are concentrated at the surface and peak of the ripple. Large pumice,

up to 2.5 $\times$  the size of associated lithic fragments, is loosely concentrated on the lee of the bedform. No evidence of slip faces were found in the sections we made, confirming that these bedforms are indeed ripples and not dunes. Given their apparent breadth and height and extreme grain-size character, we refer to these as megairipples.

Gravels can be organized by clast number density and bedform type. In some areas, disseminated gravel clasts are found (Fig. 6C), while in others, well-sorted patches of varying clast number density (Fig. 7A), incipient bedforms with sand-sized material trapped within (in eastern CPP, westernmost LP, and the eastern SI; Fig. 7B), and mature bedforms (in LP, SI;

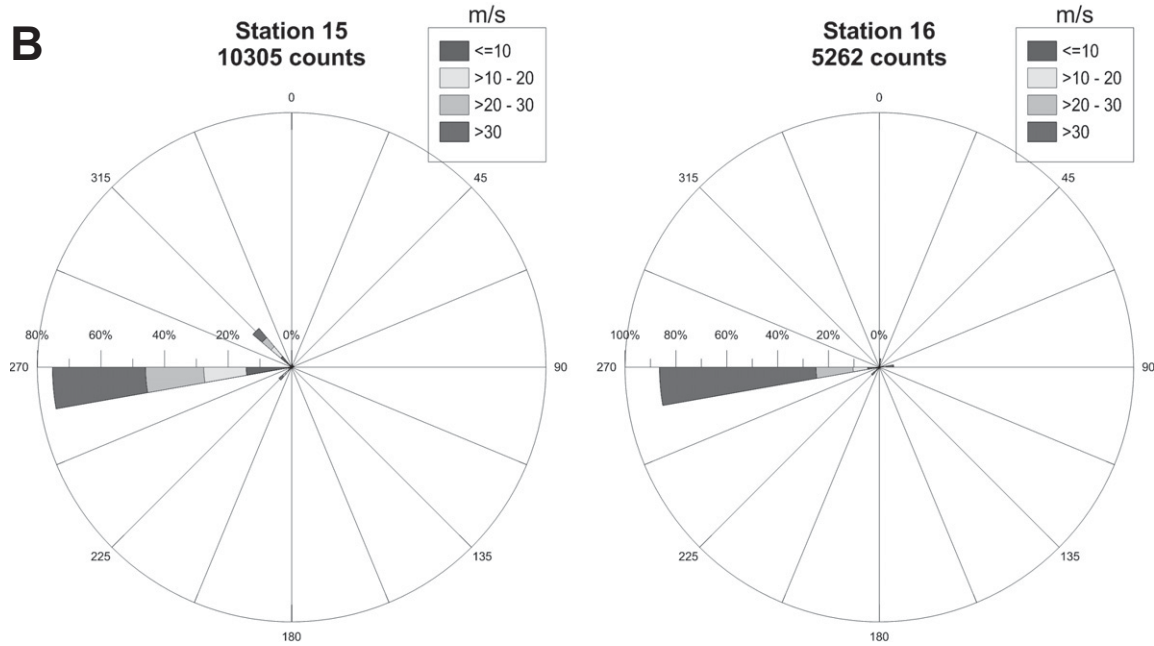


**Figure 2 (continued).** (B) Wind directions and speeds recorded at the two stations. The number of counts refers to the total number of measurements, approximately three per day at 0800, 1400, and 2000 each day. Approximately nine years of data for station 15 and five years for station 16 are included.

Figs. 3A, 3C, 7C, and 7D) are found. The largest areal extent is formed by extensive gravel bedform fields with a well-developed desert pavement (most of the CPP and LP) (Figs. 3B and 3D). We see this as a progression in maturity of the surface, with the disseminated clasts being the most immature and the broad gravel pavements being the most mature and stable.

The “immature” areas are the most instructive as they reveal the evolution of gravel bedforms. Here the post-yardang erosional surface of the ignimbrite substrate is distinctively wavy and scalloped due to differential vapor phase induration and associated differential erodibility (de Silva and Bailey, 2011). This produces a meso-scale topography at the 1–2 m vertical and 10 m horizontal scale (Fig. 6A). During the erosion of the ignimbrite, its lithic, pumice, and crystal (quartz mainly) cargo is released while the ash matrix is deflated away (Figs. 6B and 6C). Eroding ignimbrite with lithic and pumice “popsicles” (fingers of ignimbrite with the gravel clast at the tip, shielding the material behind it from sand abrasion) reveals the final stage before a lag of dispersed lithics (Figs. 5B and 5C), pumice, and crystals forms on the erosion surface. This lag begins to organize into patches in the swales or troughs between yardangs and then evolves into areally extensive sheets of dense lithics and pumice that act as particle traps. These show a progression to diffuse lenses and eventually distinct bedforms (Figs. 7A and 7B). The best-developed bed-

forms are on upslopes or the crests of the surface topography, although bedforms at various stages of development are also found on subdued ignimbrite surfaces (Figs. 7C and 7D).

### Gravel Componentry

Population statistics of the lithic components (componentry) in the gravels and the local ignimbrite were compiled to verify that the gravels originate from substrate ignimbrite (Table 1). Statistics compiled on the basis of 300 clasts visually analyzed (under hand lens and binocular microscope) and classified per sample show that the diversity and proportions of the lithic clasts in the ignimbrite and those in the gravels are remarkably similar. The ignimbrite of the CPP has more lava and vitrophyre clasts than the CP and SI fields, which in turn have a higher content of local basement Rosada ignimbrite clasts. This is consistent with the common characteristic of ignimbrites to contain a significant locally derived load through eruptive reaming of the conduit or picking up lithics from the surface over which the pyroclastic flows traveled (de Silva, 1989; Cas and Wright, 1992). Thus the lithic loads in ignimbrites are themselves locally derived. At the edge of the fields, the lithic population released from the ignimbrite can be augmented by local influx onto the ignimbrite surface. This is particularly the case in the small field of CP, where the dominant lithic is the Upper Miocene

Rosada ignimbrite, but a significant fraction of plutonic and metamorphic basement clasts are found. These lithics are sourced from both the deflating “host” Purulla ignimbrite which incorporated them as exotic lithics when it was transported and deposited in this area, as well as from the basin-flanking outcrops of the Rosada ignimbrite itself. To test the relative contributions from “basement” highs and the ignimbrite itself, components were measured from gravel bedforms at the edge of the field and from the central part that is less influenced by flank inputs. It is clear that the component from the basement is strongly enriched in the gravels on the edge of the field and is diminished in the central part of the field, confirming the “local” sourcing of ignimbrite. Pumice is derived from the local ignimbrite exclusively. The gravels are thus locally derived and were available as a lag on the surface of the host ignimbrites as starting material for bedform development.

### Wind Profile Measurements

Wind profile measurements were conducted in the CP and CPP fields during the first week of December 2010. Three anemometers were set up at logarithmic spacings up to 1.6 m. Winds in excess of  $33 \text{ km h}^{-1}$  at 1.6 m were regularly measured throughout the day. A semi-log fit to the profile data shows a roughness height ( $z_0$ ) of 1–2 cm for a range of free-stream wind speeds and field conditions from all fields except LP

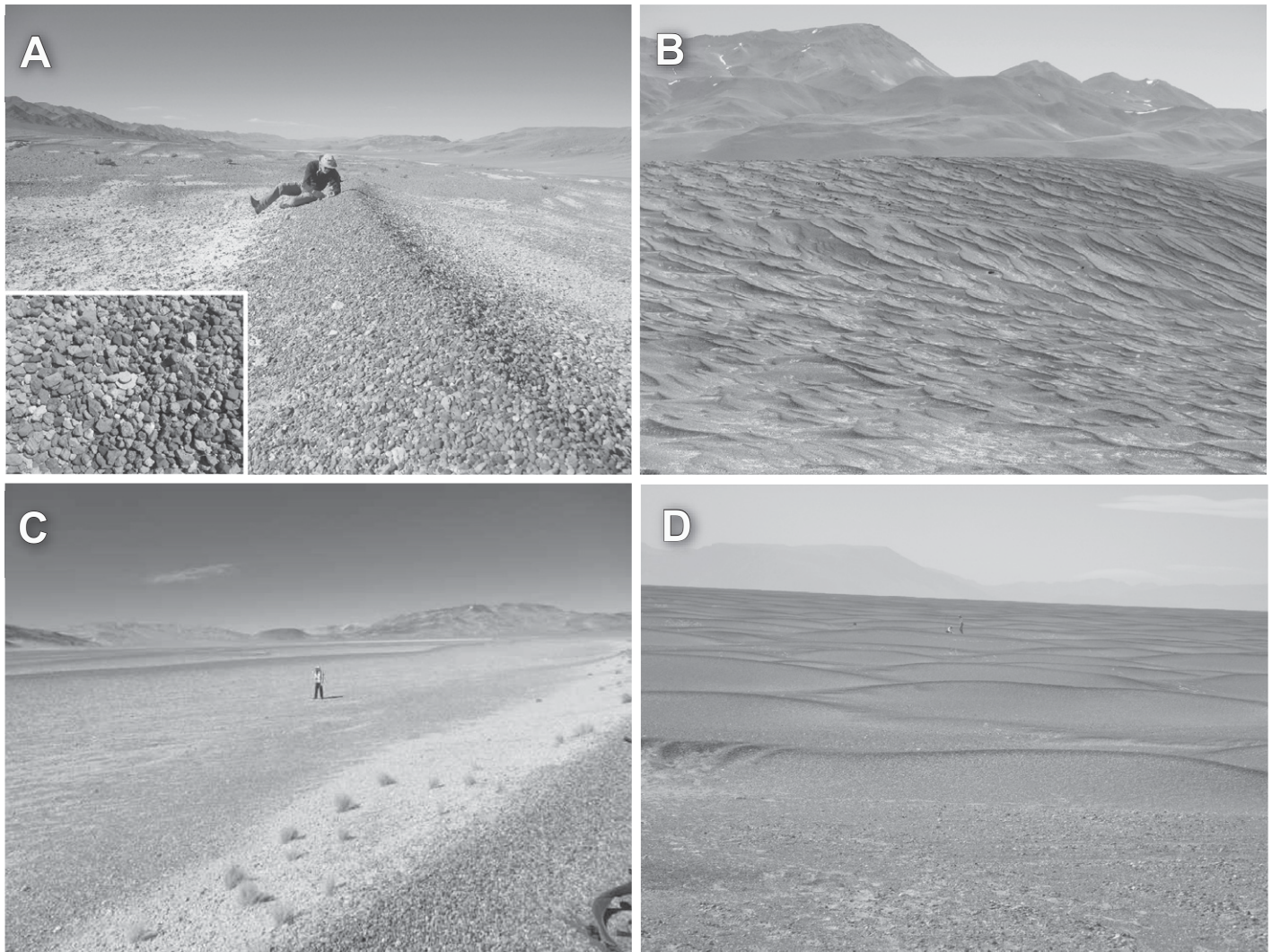


**Figure 3.** (A) Coarse gravel megaripple bedform in the Salar de Incahuasi field. Inset shows detail of the gravel on the ripple crest with 2 cm washer and nail for scale. (B) Dark gravel bedforms of the Laguna Purulla field. Typical amplitudes vary from 10 cm to 1 m and wavelengths up to 10 m. Here, interaction with topography produces a complex array of climbing ripples and interference bedforms that vary in amplitude and wavelength with proximity to topographic highs. (C) Large lithic-dominated gravel megaripple bedforms of the Campo Purulla field. The strongest winds come from bottom right. Note concentration of large pumice on the lee side of the bedform and relative stability of this face where plants have taken root. Amplitude of the topography is ~2 m and the wavelength is almost 30 m. Person for scale is standing on the substrate Purulla ignimbrite surface in the troughs between the crests formed by the bedforms. View to southeast with Cerro Blanco and La Hoyada forming the distant horizon. (D) Dark gravel bedforms in the Campo Piedra Pomez. Amplitudes of the features are ~1 m with wavelengths between 10 and 15 m.

(where wind profiling was not carried out). The derived roughness heights are thus similar to typical gravel sizes at the ripple crests. Friction speeds ( $u_*$ ) observed during our fieldwork were below that needed to move pumice. This is consistent with our qualitative observations that local sand was constantly saltating, small pumices were rolling, and silt was being suspended throughout the day. No large clasts were moving, indicating conditions were below threshold for the major megaripple components. However, conditions above threshold are common

throughout the year (Fig. 2) and particularly during the Austral winter. This is consistent with changes seen in our time-lapse imaging.

#### Time-Lapse Imaging

Time-lapse cameras were placed at three locations in the CP, SI, and CPP fields. However, only one camera, anchored on a coarse-grained ripple at the SI field, worked over a long enough time span to return interesting data. It took pictures every 2.875 (–50%, +100%) hours

over ~9–10 months (image time-tagging was not automatic, but was reconstructed later). Comparison of images acquired in December 2010 and ca. July 2011 show displacement, removal, and addition of clasts up to several centimeters in size. Most of these look like pumice (Fig. 8).

#### Wind Tunnel Experiments

To explore threshold wind speeds and provide much-needed empirical data, experiments were conducted at the Arizona State University wind

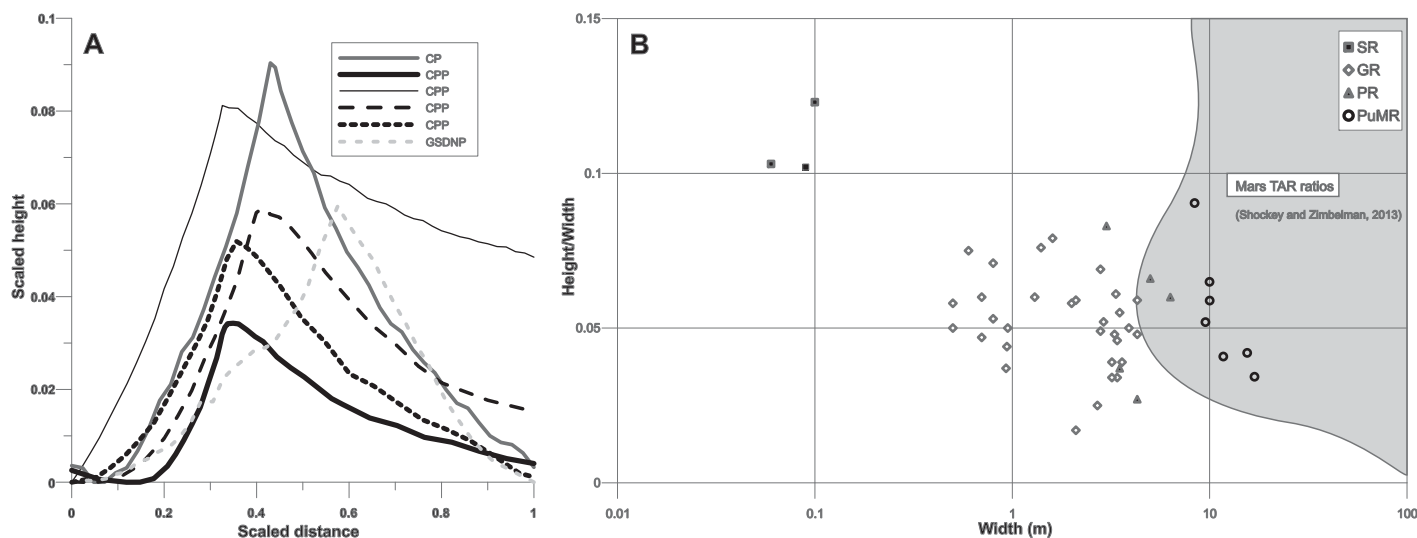


**Figure 4.** (A) Normalized profiles across gravel megaripples at Campo Purulla (CP) and Campo Piedra Pomez (CPP) fields and granule ripples at Great Sand Dunes National Park (GSDNP, Colorado, United States) for comparison, where both height and width are scaled by feature width (modified from Zimbelman et al., 2012). Note the distinct difference in the symmetry of the ripples at CP versus CPP where the ripples are clearly asymmetric. (B) Scatter plot of feature height scaled by feature width, shown as a function of feature width using a logarithmic scale. Note the distinctive shift in the Puna megaripples (PuMR; this study) toward larger values in width with respect to the same aspect ratio of other megaripples reported by Zimbelman et al. (2012) (SR—sand ripples; GR—granule ripples; PR—pebble ripples). In size and aspect they are essentially the same as small transverse aeolian ridges (TARs) on Mars characterized by Shockey and Zimbelman (2013).

tunnel in January 2012. It operates at standard pressure and temperature, with a fan and motor system able to achieve free-stream winds up to  $30 \text{ m s}^{-1}$  (~67.5 mph). It has dimensions of 13 m (length)  $\times$  1.2 m (width)  $\times$  0.9 m (height). An upwind motorized hopper can drop sand into the wind stream. The test section was coated with a surface with fine sandpaper (average grain size =  $120 \mu\text{m}$ ). Upwind, the tunnel is smooth plywood. Fluid and impact threshold were simulated, with the latter using quartz and scoria sand dropped from the upwind hopper to simulate saltating sand and pumice respectively. Details of our wind tunnel findings will be reported in a separate publication but we focus here on first-order measurements of *relative* threshold wind speeds of various field materials. As wind speed was gradually ramped up, threshold stages (vibrating, rolling, saltating) were noted, with simultaneous side-mounted video and overhead time-lapse imaging. Data are scattered (Fig. 9), but some general trends important for this contribution are apparent even from the fluid-only experiments (e.g., with no fine-grained saltating material introduced into the test section).

(1) Fluid velocities required to initiate behavior increase with clast size.

(2) For a given size range, pumice clasts vibrated, rolled, and saltated successively, whereas lithics were limited to vibration and rolling.

(3) Thresholds for pumice clasts are lower than those for lithics.

(4) Large pumice grains are capable of being transported in saltation.

(5) Vibrating and rolling of lithics of all sizes were initiated without requiring the impact of pumice.

(6) Creep and reptation (Anderson, 1987) of lithic clasts are triggered by large pumice impact.

During sand and scoria saltation experiments, rolling and saltation thresholds were much lower than in the fluid-only experiments, and lithic saltation was common once impacted by saltating sand (small lithics) and saltating pumice (large lithics). We also documented clear material segregation and clumping into ripple-like forms during sand saltation experiments. Gravel patches acted as sand traps, and we observed sand sinking through the gravel as lithics and pumice vibrated. This entire spectrum of behavior was observed at wind speeds below  $15 \text{ m s}^{-1}$  (~54  $\text{km h}^{-1}$ ) during fluid-only experiments and at lower thresholds during sand and scoria saltation experiments. These wind velocities are well within the daily averages seen in the Puna and well below the maximum winds that blow in the region. The conditions for significant aeolian work on the gravels appear to be present throughout entire year.

## DISCUSSION

Our observations provide important constraints on megaripple formation conditions in the Puna. Most significantly, we find that large pumices and lithics can move at normal wind speeds that occur in the region. If the time-lapse 2010–2011 images are representative, gravel movement is an ongoing process and is probably most effective in the winter. These data provide vital support to the deposit characteristics and observations about various stages of gravel bedform evolution derived from field observations and wind tunnel experiments and provide a model of origin, formation, and growth of the megaripples.

### A Model for the Origin of the Coarse Gravel Megaripples in the Puna of Argentina

Locally there is abundant evidence that the gravels that constitute the megaripples are a lag material that developed on the eroded ignimbrite bedrock surface. This is supported by provenance that shows that the gravels originated mainly by erosion of the bedrock ignimbrite, augmented locally by input from surrounding highlands. Additionally, the strong association of the discrete megaripple bedforms with local ignimbrite surface topography

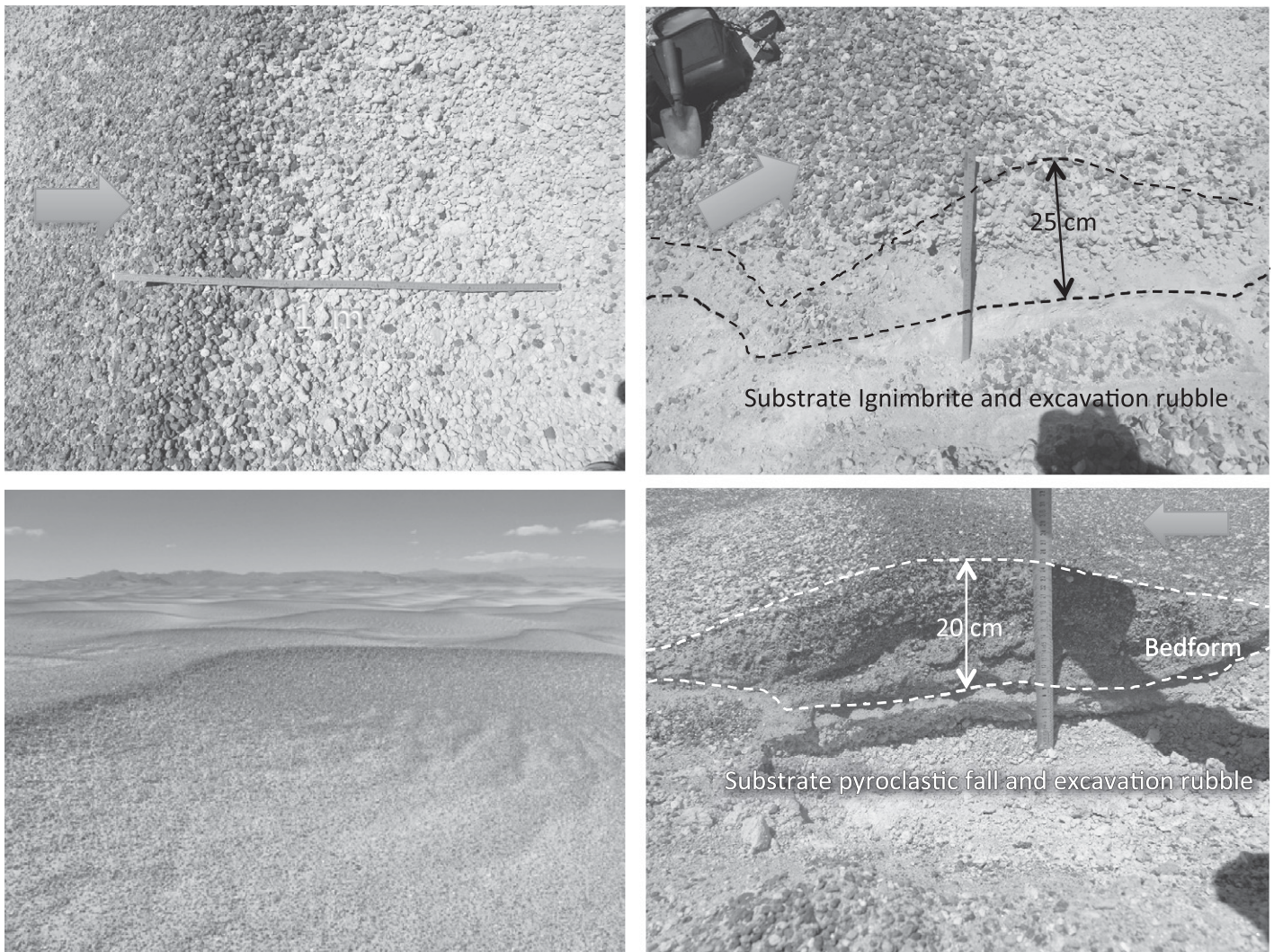


**Figure 5.** Trenching reveals that the aeolian bedforms form at the crest of the topography with the largest bedforms being ~30 cm in height above the bedrock ignimbrite. The upper 20 cm is dominated by crudely bedded coarse gravels while the lower portions are sand/silt-rich. Coarsest particles concentrate at the surface and peak. Details of gravel ripples at Campo Purulla (top row) and Campo Piedra Pomez (bottom row) showing the relation between the ignimbrite bedrock and the gravel bedform. Note the distinct crest of dense lava and basement lithics of  $\sim 2.4 \text{ g cm}^{-3}$  and the lee-side accumulation of less-dense pumice of  $\sim 0.8 \text{ g cm}^{-3}$ . Pumice sizes range up to 6 cm whereas lithics up to 2.5 cm are found. Scale is 1 m.

and pumice clasts with the gravels suggests that organization of the gravels into bedforms was influenced by these two factors. The concentration of pumice clasts on the lee side of the bedforms implies a symbiotic relationship between gravel bedform development and pumice accumulation.

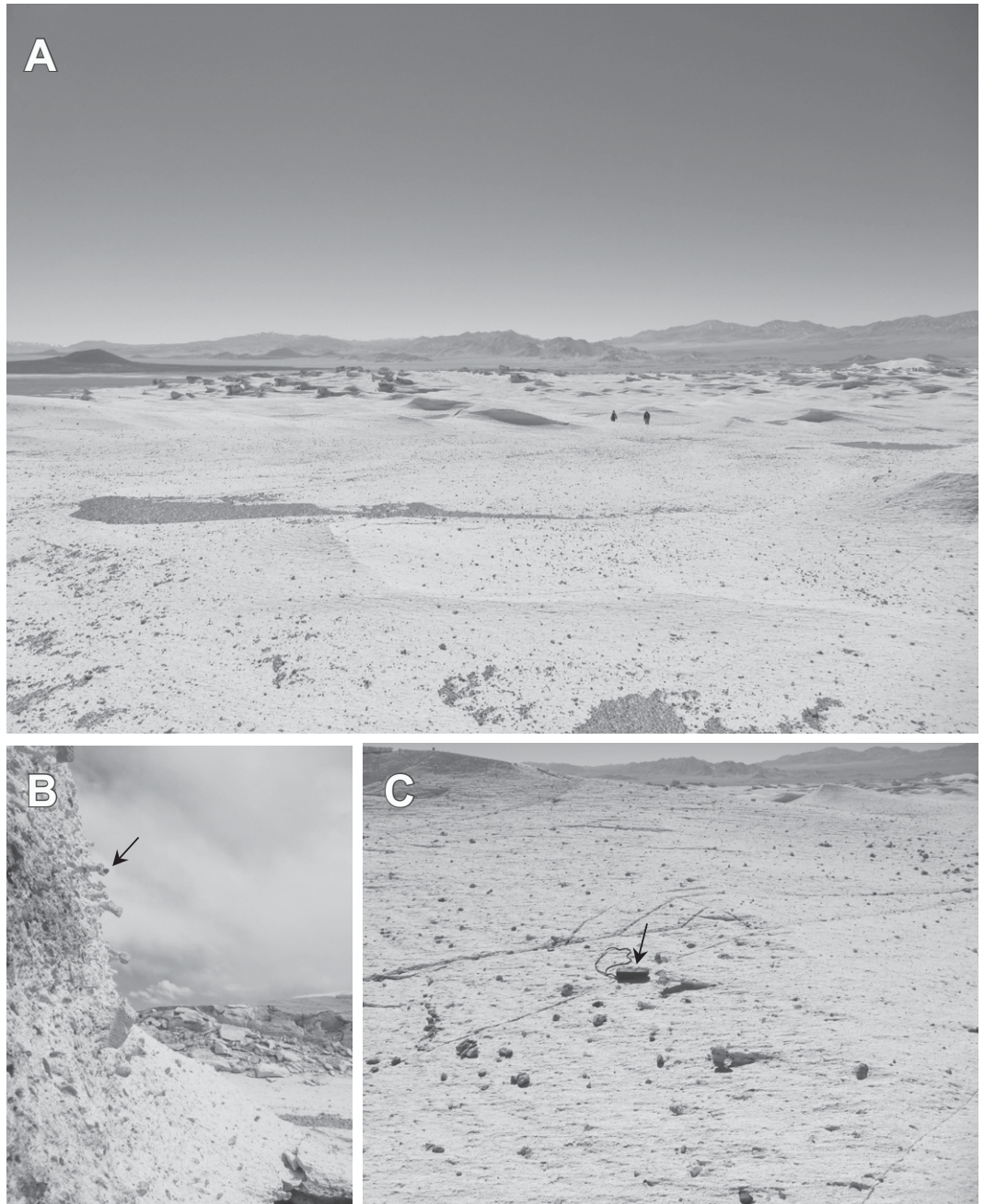
We suggest that saltation of pumice and sand results in creep of gravel through impact energy transfer. This was observed in our wind tunnel experiments where large pumice clasts up to 7 cm saltated effectively at wind velocities of less than  $13 \text{ m s}^{-1}$ , and as low as  $7 \text{ m s}^{-1}$  with saltating sand and scoria. Adjusting for the approximate atmospheric density differences

between Tempe, Arizona ( $\sim 400 \text{ m}$  elevation), and the Puna at  $\sim 4500 \text{ m}$  elevation gives equivalent velocities in the field of 17 and  $9 \text{ m s}^{-1}$ , respectively (e.g., for 273 K, the scale height is 8 km, such that the density ratio between Puna and Arizona will be  $\exp(-4.1 / 8) = 0.6$ ; the threshold friction speed is proportional to the square root of this value, so will be  $\sqrt{1 / 0.6} = 1.3\times$  greater in the Puna). Isolated flat-aspect (discoïd) pumice clasts as large as 5 cm saltated even in fluid-only experiments, depending on facet orientation to the wind. Impact of saltating sand and pumice initiated rolling of lithic clasts (creep) and impact of large 5 cm saltating pumice initiated saltation of 2 cm lithic fragments.

Creep is therefore the most likely transport mechanism for the Puna gravels.

The viability of creep in the Puna gravels may be evaluated by inverting their grain-size characteristics (e.g., Jerolmack et al., 2006). Following Bagnold (1941), impact of saltating 1–3 cm pumice clasts found in the Puna gravels should be able to induce creep in 1–2 cm andesite clasts. Simple calculations yield threshold friction velocities ( $u_{*t}$ ) for 1–3 cm pumice grains of  $1.17\text{--}2.0 \text{ m s}^{-1}$  (Shao and Lu, 2000) or  $1.3\text{--}2.2 \text{ m s}^{-1}$  (Greeley and Iversen, 1985) using a particle density of  $800 \text{ kg m}^{-3}$  and an atmospheric density of  $0.7 \text{ kg m}^{-3}$  appropriate for 4500 m elevation. Using a friction speed of

**Figure 6.** (A) Campo Piedra Pomez looking north; Carachi Pampa cinder cone in center left. Ignimbrite is being stripped by aeolian erosion into yardangs that are eventually stripped off to leave a scalloped surface. Dark areas are gravel that is collecting within the scallops. People in middle distance for scale. (B–C) The aeolian erosion results in abrasion and deflation of the ignimbrite ash matrix, releasing lithics and crystals into a lag that develops on the deflated surface. This process continues until aeolian efficiency is limited by the deflated surface. Arrow in C points to a lithic clast that is 3 cm in the view. Arrow in D points to GPS unit that is 7.5cm long in this view.



$1.17 \text{ m s}^{-1}$  (the minimum using the Shao and Lu equation), a roughness height of 5 mm, and taking von Karman's constant as 0.4, the predicted threshold wind velocity (at 2 m height above the bed) is  $(1.17 / 0.4) * \ln(2 / 0.005) = \sim 17.5 \text{ m s}^{-1}$ . These velocities are consistent with the peak sustained wind velocities of 20–30  $\text{m s}^{-1}$  (at a height of 2 m) measured in the month of July in this region, and are in the range of the thresholds we observed in our wind tunnel experiments ( $\sim 19.6 \text{ m s}^{-1}$ , with the wind tunnel results scaled to the difference in atmospheric density). All these estimates indicate that dis-

persed gravels can be effectively moved and concentrated into bedforms under regular conditions in the Puna.

We integrate all these considerations into a model for the origin and formation of the gravel megaripples, summarized in Figure 10. Disseminated gravel released from the eroding ignimbrite and yardang formation as described by de Silva et al. (2010) is the point of departure.

(1) Saltating sand and pumice (locally derived) cause the lithics to creep and maybe (for the smaller sizes) even saltate and reptate (Fig. 10A).

(2) Saltation of sand and pumice continues throughout the process, deflating the ignimbrite and causing the yardangs to recede and release more lithics, pumice, and crystals (Fig. 10B).

(3) The undulating topography on the post-yardang ignimbrite surface serves to focus the accumulation of gravels, with the upslope acting as an energy barrier to all but the most energetic clasts that may top the crest and roll into the next low and join the next bedform. Bedforms may also nucleate on flat surfaces if a stable concentration is locally facilitated by any of the abun-

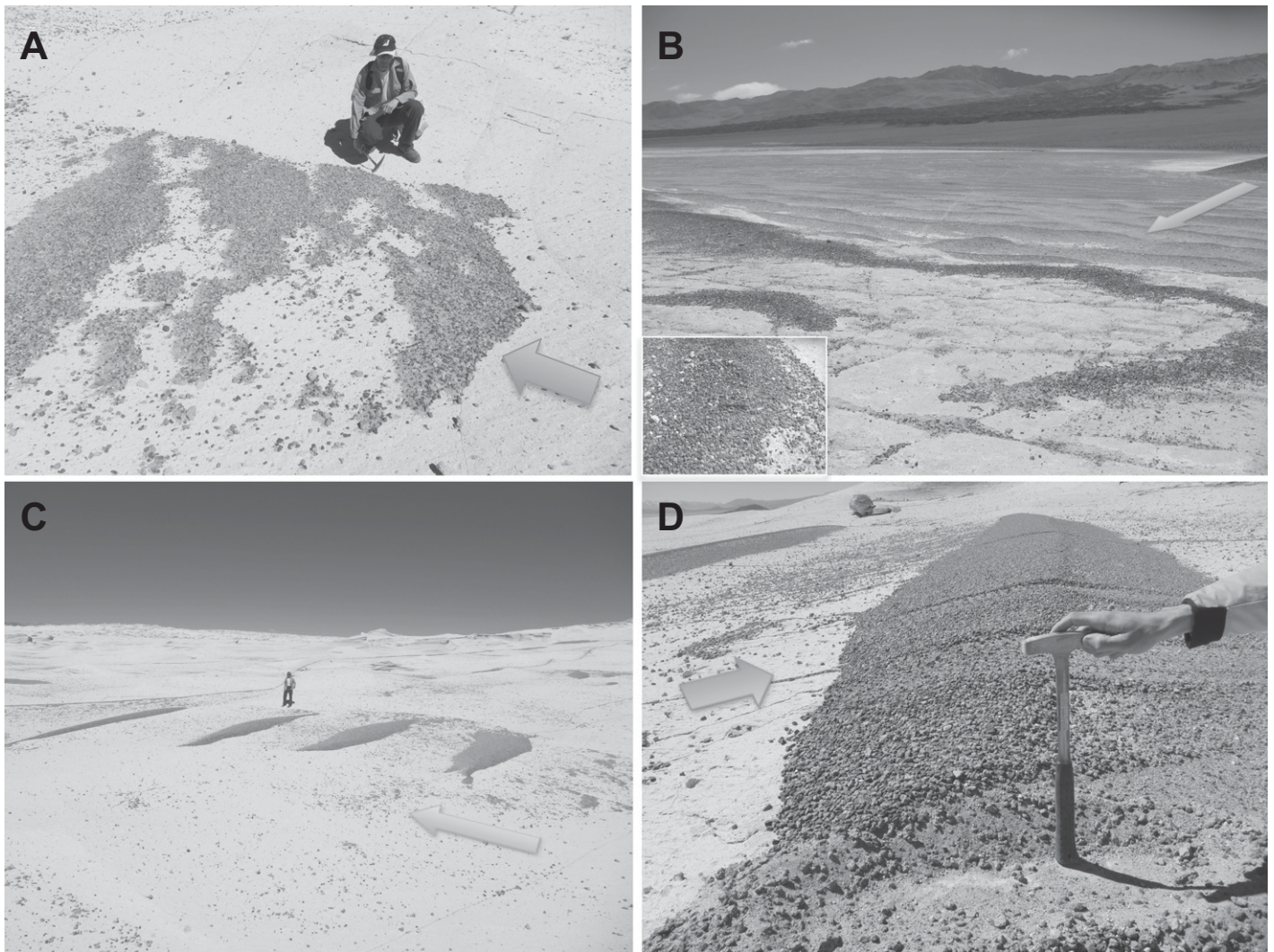


**Figure 7.** Sequence showing the evolution of gravel bedforms. Wind direction shown by large arrow. (A–B) Gravels organizing into incipient bedforms at Campo Piedra Pomez (CPP) (A) and Laguna Purulla (B). Gravel acts as sand and silt traps, whereas the ignimbrite surface is stripped clean. (C) Periodic bedforms on CPP form at local topographic highs. (D) Excavation of a dark megaripple from the area shown in C. Core of the ripple is structureless sand, with the outer surface formed by the armor gravel of dominantly lithics with pumice accumulated mainly on the lee side (right).

dant centimeter-scale perturbations that could act as local barriers to movement.

(4) Once bedforms nucleate and accumulate, they stabilize, as the closely packed gravel is difficult to move. The most extensive bedforms appear to nucleate on the local dominant “high,” setting up a feedback between the bedform, airflow, and lee-side accumulation of saltating pumice.

(5) Interference by the prominent transverse gravel bedform results in significant perturbation of the wind field. A lee-side wind shadow zone that allows pumice to concentrate and remain protected probably forms. Flow separation over the bedform may result in streamline compression, expansion, and reversal (e.g.,

Jackson et al., 2011, 2013; Delgado-Fernandez et al., 2013; Smyth et al., 2013) and lead to vortices that deepen the troughs through impact erosion by fine sand and saltating large clasts (larger particles likely cannot be entrained in vortices) and deflation.

(6) The stabilized “bedform” is thus an equilibrium form that is only modified if disrupted during rare extreme conditions. Thus, under normal conditions for the Puna, we envisage that once established, the position of the megaripples remains relatively constant, with clasts periodically removed from one megaripple and then saltated downstream onto another as observed in our time-lapse photography. This probably reflects limits to growth due to two compli-

mentary mechanisms (Isenberg et al., 2011): (a) as the bedform grows, increasing shear stress at the crest reaches a critical threshold that will entrain particles from the crest; and (b) as wind speed increases, higher saltator impact speeds may remove coarse grains from the crest.

Therefore, these are not ripples in the sense of migrating bedforms, but rather nucleation sites of wind-transported sediment. The life of a typical particle would therefore consist of quick hops between the ridges, followed by long-term stability at the “ripple” locations.

Thus, overall we see an evolution of the surface of ignimbrite bedrock → yardangs → gravel sheets on undulating bedrock → gravel bedforms on bedrock ridges → stable mega-

TABLE 1. GRAVEL AND SUBSTRATE IGIMBRITE MATRIX COMPONENTRY EXPRESSED AS PERCENTAGE OF POPULATION BASED ON 300 CLASTS PER SAMPLE

	Igimbrite matrix	Gravel	Igimbrite matrix	Gravel
<b>Campo Piedra Pomez</b>				
(n)	<b>23</b>	<b>3</b>		
Vitrophyre	8	10		
Igimbrite	74	70		
Andesite	5	7		
Metamorphic	13	13		
<b>Campo Purulla</b>				
(n)	<b>West</b>		<b>Central (further from basement)</b>	
	<b>11</b>	<b>4</b>	<b>4</b>	<b>2</b>
Rosada ignimbrite	25	21	29	30
Other ignimbrite	19	15	20	18
Andesite	15	13	14	16
Vitrophyre	30	20	25	21
Basement	11	31	12	15
<b>Salar de Incahuasi</b>				
(n)	<b>5</b>	<b>3</b>		
Rosada ignimbrite	33	44		
Other ignimbrite	12	13		
Andesite	18	13		
Vitrophyre	12	10		
Basement	25	20		

ripples capping the dominant local highs. This may evolve to deepening of troughs and lengthening of ridges with time, possibly leading to the large mature ripple-capped topography at Cerro Purulla and gravel pavements of CPP and LP.

### Growth of Megaripples

The cores of the megaripples are dominantly a mix of sand and silt (<125 mm), while the mantle gravels lack sand. This poses a conundrum. Conditions that lead to the movement and deposition of gravels are inconsistent with deposition of sand-sized and finer material. Indeed our observations are that most sand is transported out of these basins and deposited to the east in massive dunes and sand fields. Finer material is suspended and transported east into the Argentinean Pampas where thick loess deposits are dominated by ash from the Cordillera (Teruggi, 1957; Hepper et al., 2006). It is telling that there is almost a complete lack of bedforms consisting of sand in any of the basins that have gravel megaripples. In open areas, sand is found only in sheltered locations or where trapped within locales dominated by gravel. The only significant accumulations of fine material are capped by gravels and attain thicknesses of 20–30 cm in crests of the megaripples. Therefore, we propose that the transport and deposition of gravels is decoupled from the sand and finer material, with the gravels, once formed, acting as aeolian traps because they (1) have high initial surface roughness that cause local reduction in near-surface wind velocities and concomitant deposition of fines and (2) high permeability that limits surface run-off and erosion and enhances the likelihood of entrapment of fine material.

This is consistent with the wind tunnel experiments. Under all three experimental conditions

(fluid, saltating sand, saltating scoria), the only sand that remained within the tunnel at the end of each experiment was that trapped in the gravel. Furthermore, the silt and sand deposited on top of the gravel was eventually moved downwards through the gravel as agitation and shaking of gravel clasts resulted in kinetic sieving of the fine particles.

These observations lead us to propose that the fine-grained cores of the gravel megaripples are trapped sand and silt that infiltrated and percolated downward. Rather than a sequential deposition of sand-dominated bedforms (of which there are none in the present day) that are later overrun by gravel deposition, or have simultaneous deposition of fine material and gravels in a complex saltation curtain (Milana, 2009; Milana et al., 2010), we suggest that sand trapped by the gravel ripples is gradually kinetically sieved downwards, undermining the gravel and “lifting” the gravel armor upwards to form a gravel-mantled bedform (Fig. 11). Kinetic sieving results from “wobbling” or “agitating” gravel clasts, a common occurrence based on our wind tunnel observations. Freeze-thaw may also seasonally affect the permeability of the gravel, and melting snow or frost or rare rain may also facilitate downward transport through the permeable gravel. In this way a nascent unimodal gravel bedform grows and develops a bulk bimodal grain-size distribution where the surface mantle is many times coarser than the finer-grained core. Some mixing of gravel downwards is expected, as the sieving process may not be completely efficient. Internal layering, such as rare internal sandy beds, would

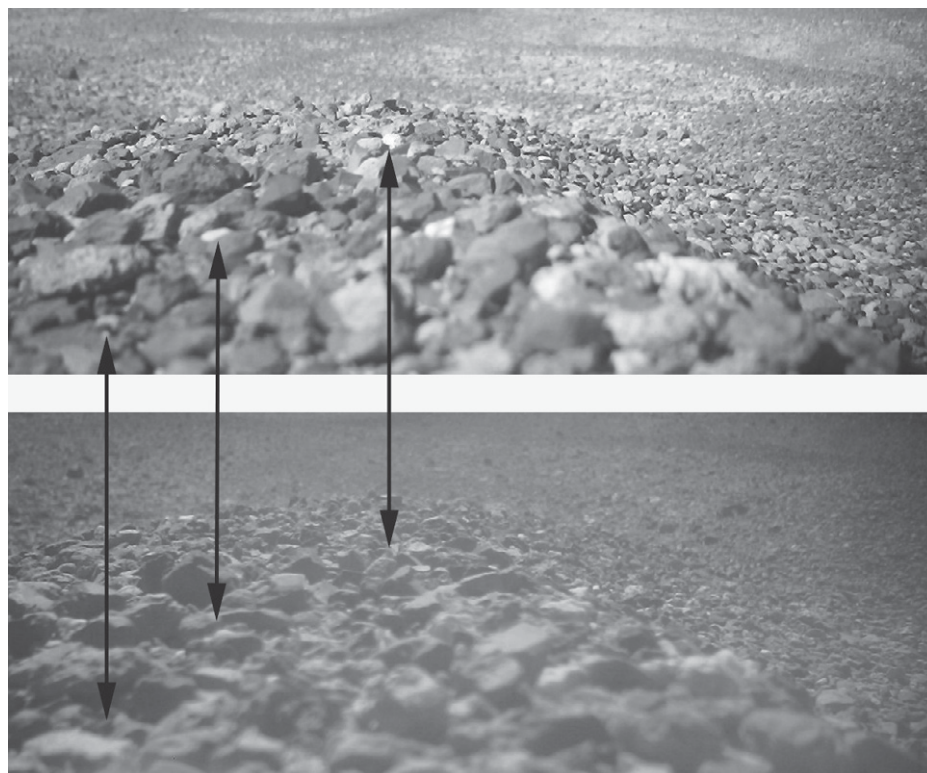
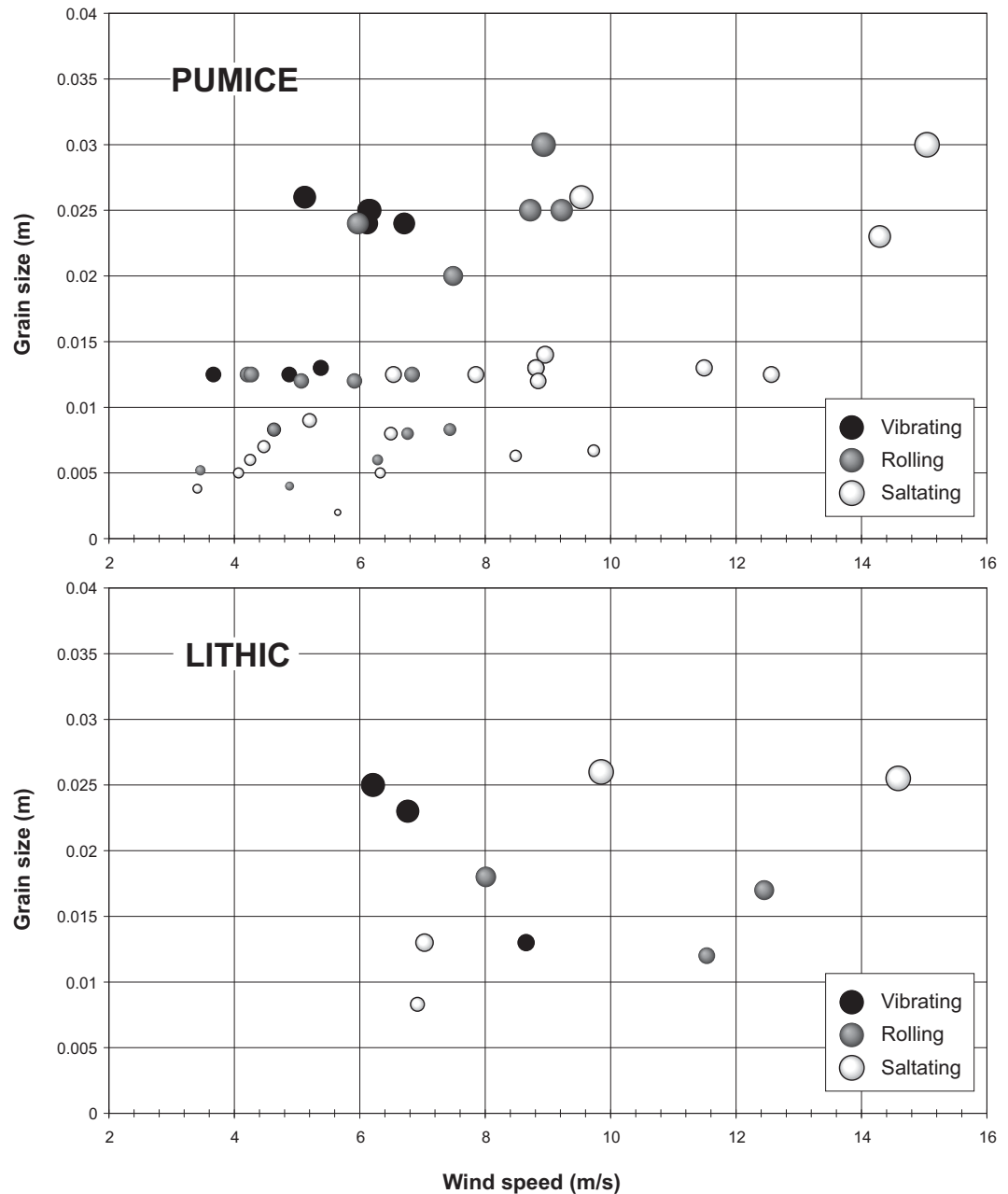


Figure 8. Removal and addition of large pumice fragments as seen in time-lapse images acquired in December 2010 (top) and ca. July 2011 (bottom) at the Salar de Incahuasi site (26°30.865'S, 67°42.053'W). Arrows point to some changes in clasts between the two images.

**Figure 9. Preliminary results of wind tunnel experiments showing threshold behavior of Puna gravel materials. Plot shows fluid velocities measured in the wind tunnel against clast size for pumice (density = 1.2 g cm<sup>-3</sup>) and lithics (density = 2.4 g cm<sup>-3</sup>). Each sphere in the plot represents one clast, with shades representing different behavior observed and logged during analysis of videos of the experiments.**



implicate ephemeral sand sheets swept through the area. Rare internal gravel-rich beds may indicate a stable mantle that was subsequently buried by a new cycle of gravel deposition, infiltration, and growth.

A role for the “shadowing” process described by Sharp (1963) is also suggested. As the megariipple grows, the coarse particles at the crest shadow or protect the lee side. The megariipple grows in height, width, and wavelength as more coarse particles creep up the stoss (windward) side and pile up at the crest. The increasing crest height shadows an increasing length on the lee side from incoming saltating sand (not all of it,

but probably the fastest ones that are moving at a very shallow angle relative to the regional slope) allowing pumice to accumulate there.

**Comparison with Previous Work**

Although more extreme than megariipples so far described on Earth, the Puna megariipples may not be unique (e.g., Zimbelman et al., 2012; Yizhaq et al., 2009, 2012). In their early discussion of megariipples, Greeley and Iversen (1985) referred to reconnaissance observations from northeast Iceland (Greeley and Peterfreund, 1981) where bimodal megariipples with

wavelengths of up to 7 m and amplitudes of 25 cm can be found. Interestingly these megariipples consist of light-toned, low-density pumice 1 cm in diameter, and dark denser obsidian clasts 0.75 cm in diameter. Greeley and Iversen (1985) recognized that a bimodal density distribution was probably a required condition for the formation of coarse megariipples. They posit that under wind conditions that were too light to move large clasts, but sufficient to saltate finer grains, impact of saltating grains induced creep in the larger grains. In this way a lag concentration of coarse grains on the surface was organized into bedforms to form megariipples. This

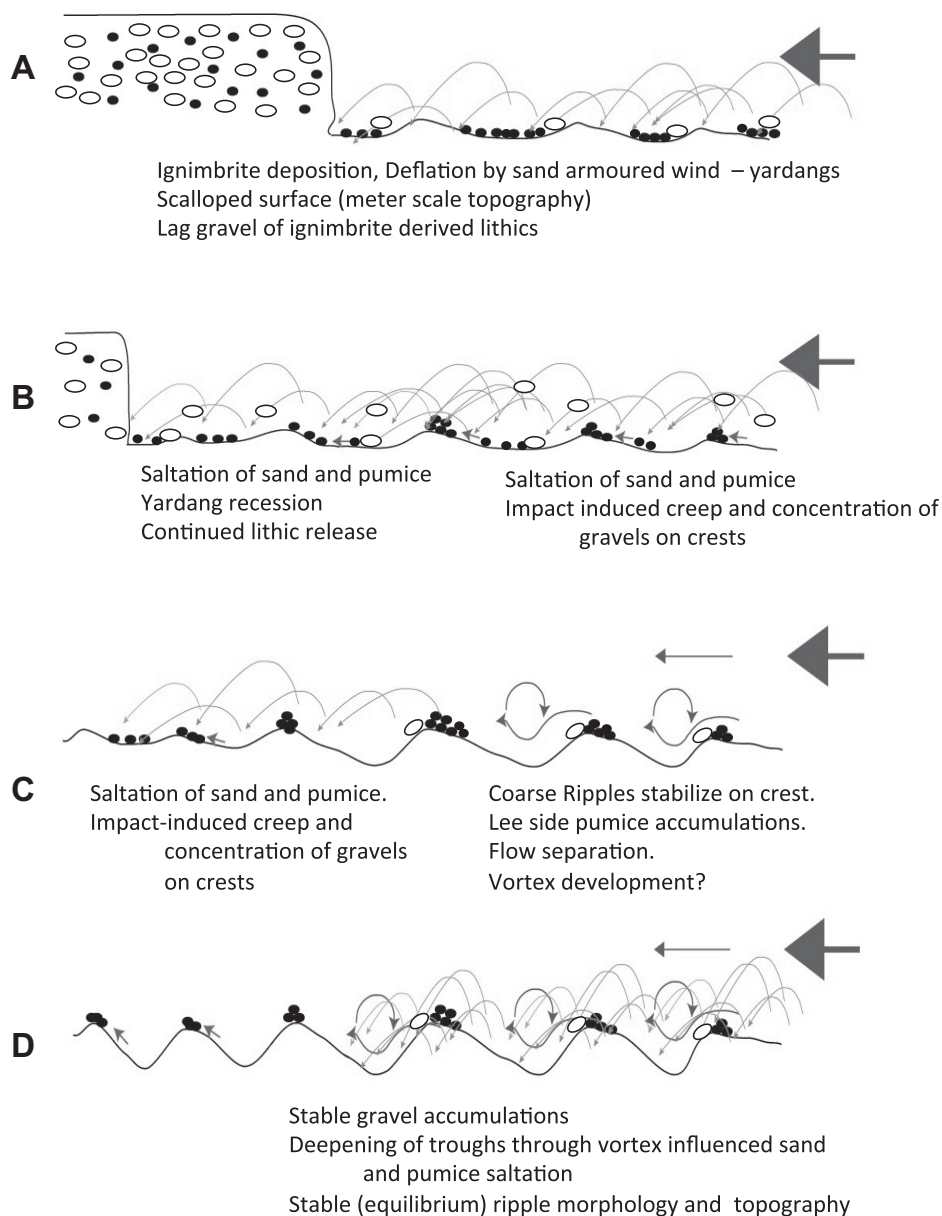


**Figure 10. Conceptual diagram illustrating the relationship between ignimbrite deflation, yardang formation, and gravel bedform nucleation. Details of the yardang formation process are explained in de Silva et al. (2010). Open ovals—pumice; black ovals—lithics.**

is consistent with what we see in the Puna, albeit at more extreme clast sizes and densities, implying stronger wind conditions.

Aeolian gravel bedforms from the Dry Valleys of Antarctica provide a valuable comparison (Selby et al., 1974; Ackert, 1989; Gillies et al., 2012). A variety of gravel megaripple forms are described and as a group they are quite variable, some being strongly asymmetric. They share characteristics with aeolian sand ripples and megaripples, but also have features unlike any of those forms (Gillies et al., 2012).

They are all interpreted to have formed by intermittent creep induced by, in this case, saltating sand grains. However, unlike the Puna examples herein, they are not connected, repetitive bedforms, do not contain a bimodal clast population, and are not as coarse nor as large. Nonetheless, the megaripple forms of the Asgard Range described by Ackert (1989) have some important similarities to the Puna examples. These are almost as coarse as those from the Puna and the gravel pavement (armor) is underlain by a ripple core made up of a “diamicton” of sand

and gravel that overlies fine-weathered bedrock above bedrock. Individual ripples occur on local topographic highs and make up only ~20 cm of the 50 cm amplitude. Ackert’s observations that “gravel was transported upslope” (p. 61) and that “ripple formation likely began with weathering of exposed (sandstone) bedrock” (p. 62) echo our own observations in the Puna. The interpretation that “ripples are derived from reworking by wind of a weathered sandstone regolith” (p. 61) parallels our observation of the local origin of the Puna gravel clasts.

Our infiltration and accretion model for gravel megaripple growth is similar to that described by Wells et al. (1985) for the growth and stabilization of stone pavements capping accretionary mantles on lava flows in the Cima volcanic field of New Mexico. Here, trapped aeolian sand and silt gradually lift the stone pavement by infiltrating and accumulating beneath. A well-developed pavement reflects stability when the permeability is reduced by sediment accumulation and runoff is promoted. Whereas significant runoff is rare in the Puna, the extensive gravel pavement and megaripples likely have a strong resistance to aeolian disruption once established. This is the probable cause for the extensive gravel pavements of the CPP and LP fields and the extreme topography of the CP field.

Our model of growth of gravel bedforms through infiltration and accretion of aeolian sand and silt trapped in locally derived gravel accumulations and their genetic relationship to the bedrock ignimbrite is quite different from that proposed by Milana (2009) and Milana et al. (2010). Both interpretations agree that coarse ripples migrate to and develop on local crests of surface topography, however the origin of the gravels from the local ignimbrite, the sequence of nascent bedforms and their evolution to mature megaripples, the trapping of sand and silt, and the intimate association of lee-side pumice concentrations are not noted by Milana. Some of these omissions were pointed out by de Silva (2010). These are critical observations if we are to fully understand the development of these gravel-mantled bedforms.

Milana (2009) discounted a creep mechanism for the coarse gravel bedforms. We support our assertion that saltation of pumice and sand induces creep in the dense gravel clasts with the observation of the intimate association of pumice and dense gravels, the occurrence of lee-side coarse pumice concentration, and the results of wind tunnel experiments. Milana (2009, p. 345) suggested that medium- and large-scale ripples might be formed in response to “Helmholtz instabilities as a result of shear along the interface at the top of a dense saltation layer

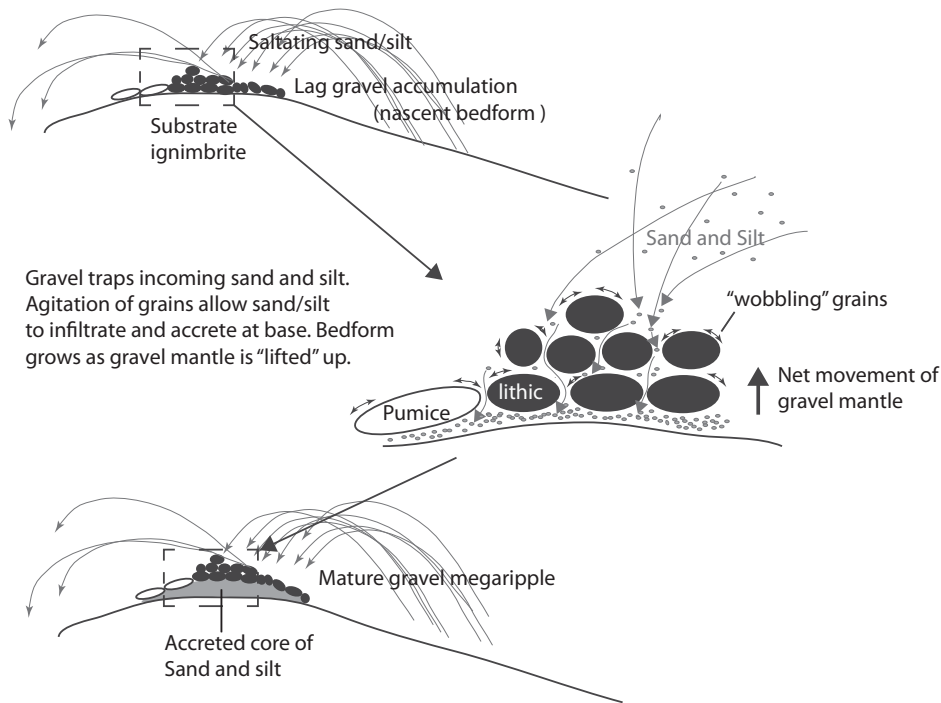


**Figure 11. Schematic representation of the infiltration and accretion model for growth of gravel megaripples in the Puna. See text for discussion.**

that behaves as a boundary layer.” Our observations are that the nucleation and development of nascent ripples is not associated with deposition of any fine material, thus evidence of a fines-dominated dense boundary layer is not present in juvenile ripple forms. Indeed all indications are that aeolian transport here is extremely efficient in fractionating different sizes and densities, with little sand and silt deposited unless trapped by gravel. Our observations lead us to the conclusion that fine material infiltrates a stable permeable coarse gravel bedform and “lifts” the coarse gravel to form a gravel-mantled, sand/silt-cored bedform.

Our model has implications for ages of megaripple cores reported by Milana et al. (2010). Specifically, we propose that the cores of the megaripples are accreted over time and not the result of a single depositional event. Milana et al. (2010) reported optically stimulated luminescence (OSL) ages ranging from  $635 \pm 45$  to 3000 years for “average” megaripples. OSL ages require a bulk sample of “light-sheltered” sediment. Under our model, such a sample would contain grains that accumulated slowly over a long period with quite different light exposure histories. A single OSL age is therefore likely to consist of some weighted mean of a complex and unknown distribution of ages. The meaning of the reported OSL ages to ripple formation rates is therefore unclear.

Nevertheless, we agree with Milana (2009) on some points. The mature megaripples of the Cerro Purulla field are quite remarkable. Our field wind experiments (to be detailed in a separate, forthcoming paper) reveal complex flow over these megaripples (e.g., Jackson et al., 2011, 2013; Delgado-Fernandez et al., 2013), with clear evidence of flow separation. We suggest that once large megaripples stabilize, wind flow characteristics coupled with continued saltation of pumice and sand act to deepen the ignimbrite bedrock troughs between the ripple crests (Figs. 10C and 10D). In this case the Purulla ignimbrite is much less indurated than the CPP ignimbrite that underlies both the SI and CPP gravel fields where such deep troughs have not developed. This is probably an important control on the evolution of the ignimbrite surface and therefore we agree with Milana (2009) that trough deepening may occur by wind flow and saltation pathways affected by the gravel bedforms (Fig. 10C), but only *after the bedforms have stabilized*. The gravel-capped-ridge-and-trough terrain of CP thus reflects a mature stable megaripple terrain that is dominated by trough modification at the present time. These ideas will be examined through further study.

Finally, if as we think, many of the largest ripples nucleate on pre-existing topography, then there is very little relationship between wavelength and classic aeolian properties (e.g., wind

speed, trajectory length). In fact, such a mechanism breaks down any wavelength scaling to aeolian processes or to ripples that form in the absence of pre-existing topography. Classification of these features is therefore complicated. However, there are some ripples in the Puna that are *not* on topographic highs. These are more relevant to comparing to other data sets. This is an area of future work we aim to explore.

This region of the Puna is a rare natural laboratory for the development of extreme aeolian sediments and bedforms. It may represent an aeolian geomorphology “perfect storm” resulting from a unique confluence of circumstances: (1) a bedrock lithology (ignimbrite) that is susceptible to aeolian erosion, (2) a resulting undulating erosional topography, (3) a readily released bimodal association of clasts with complementary aeolian behavior, and (4) a region dominated by aeolian activity. As far as we know, the confluence of these features and the feedbacks that result have not been described anywhere else on Earth.

## IMPLICATIONS FOR MARS

Do these extreme, possibly unique bedforms tell us anything about Mars? Although such coarse bedforms have not yet been described on Mars, we find several themes where our observations of the Puna gravel-mantled megaripples are relevant.

First, the Puna gravel bedforms consist of materials that have similar equivalent weight to those composing the granule ripples at Meridiani Planum, Mars. The Puna megaripples are composed of pumice of density  $0.8\text{--}1.3\text{ g cm}^{-3}$  capped by lithics with a density of  $2.6\text{--}3\text{ g cm}^{-3}$ . For a cubic centimeter of material, this translates to a weight on Earth of 8–13 and 25–29 mN, respectively. The Meridiani ripples consist of basalt ( $\sim 3\text{ g cm}^{-3}$ ) capped by hematite concretions ( $\sim 4.9\text{--}5.3\text{ g cm}^{-3}$ ; Soderblom et al., 2004), which, for a cubic centimeter of material, weighs 11 and 18–20 mN, respectively, on Mars. For such large particles, effects of particle friction Reynolds number and inter-particle forces can be largely ignored, such that material weight is the main resistive force to the wind (Kok et al., 2012). Therefore, the resistive forces for the ripple cores are about the same in the Puna and on Mars, with those for the capping materials slightly less on Mars. For equivalent weight materials, of which these more or less are, the threshold friction speed needed for movement is proportional to the square root of atmospheric density (Shao and Lu, 2000). Taking atmospheric densities of  $0.7$  and  $0.0154\text{ kg m}^{-3}$  for the Puna and Mars, respectively, results in threshold speeds that must be  $\sim 7\times$  greater

on Mars ( $\sqrt{0.7 / 0.0154}$ ). Such high-speed threshold winds occur much less frequently on Mars (Haberle et al., 2003) than they do in the Puna. Furthermore, the occurrences of excess shear stress (e.g., from velocities above threshold) are certainly much more common, and of greater magnitude, in the Puna than on Mars. Therefore, we can consider the Puna a good analog for Mars, but operative at rates that are probably much greater due to the generally higher frequency of threshold winds and both frequency and magnitude of winds above threshold. This is in large respect an advantage, as it represents Mars aeolian processes in “fast motion” that can be studied *in situ*. Taking the Meridiani values and factoring in martian gravity (0.38 that of Earth) means that a cubic centimeter of basalt on Mars has about the same weight as pumice on Earth. If we assume a density of 4.9–5.3 g cm<sup>-3</sup> for hematite, its Mars equivalent weight for a cubic centimeter would be 1.8–2.0 mN, somewhat less than the 2.6–3 mN for the exotic lithics. The Puna therefore serves as a natural laboratory for Mars. In particular, our demonstration that the bimodal clast population of pumice and lithics is critical to the development of gravel bedforms and the impact of saltating (low-density) pumice is the main driving force for creep of the denser lithic clasts may be a useful analog for the development of Terra Meridiani ripples through basalt impact on hematite.

One of our preliminary findings is that once stabilized, Puna gravel bedforms appear stable while still remaining dynamic features that experience clast exchange. Similarly, TARs on Mars have not been observed to migrate (Balme et al., 2008; Berman et al., 2011), in contrast to some dunes and ripples (Bridges et al., 2012, 2013), and it has been inferred that megariipples distal to large dunes are inactive under present conditions (Berman et al., 2011). This is perhaps an unsurprising result if TARs are indeed megariipples armored with coarse grains like those that characterize plains ripples in Terra Meridiani (Sullivan et al., 2005) and the lower frequency of high wind events on Mars relative to the Puna, as described above. In this respect, the morphologic similarity of the Puna megariipples to TARs demonstrated in Figure 4 is intriguing.

Our observations in the Puna also help reconcile current models of TARs (Balme et al., 2008; Zimbelman, 2010; Berman, et al., 2011) with the recognition that some periodic bedrock ridges (PBR) may be produced by aeolian erosion (Montgomery et al., 2012). The flow separation model presented for PBRs is similar to the model proposed here for the development of the topography after mature Puna megariipples

have formed. The presence of sediment capping some of these PBRs makes this analogy potentially even more compelling.

Second, the spatial relationships among these Puna megariipples, topography, and bedrock are analogous to relationships among TARs, topography, and bedrock on Mars. This is particularly obvious in HiRISE data that show details of TAR development in swales between yardangs in the Medusa Fossae Formation (MFF) (Fig. 12A). Here, light-toned bedrock is variously covered with bedforms, with the larger ones located on the flanks of the topography and the smaller ones in the swales. An analogous situation is seen in the CPP and SI in particular where lithic gravels derived from aeolian erosion of ignimbrite form distinct bedforms in the swales between the resulting yardangs (Figs. 12B and 12C). This analogy is made even more pertinent as the most likely MFF lithology on Mars is ignimbrite (Scott and Tanaka, 1982; Mandt et al., 2008, 2009). Our hypothesis is that these are lag gravels left when the matrix of the host ignimbrite was eroded and deflated away by the wind. If true, then the characteristics of the bedforms can tell us about the behavior of these gravels in areas of incised topography compared to more open areas where the megariipple bedforms have formed. Perhaps many or all TARs consist of eroded ignimbrite and mantles (which are common on Mars [Malin and Edgett, 2001] and for which the method of erosion and the resulting byproducts are poorly understood), thereby explaining the distinct albedo and presumed grain-size differences compared to dark sand dunes.

Third, our observation that the gravels that mantle the megariipples are locally derived has implications for the source of material in martian ripples, dunes, and TARs. Such a local derivation would obviate the need for large-scale transport of sediment as has been inferred for dark dunes on Mars (Burr et al., 2012). It may be that much dark sand elsewhere on Mars, prior to transport to its present location, could have been derived from ancient volcanoclastic mantles that have subsequently been stripped away (Edgett and Lancaster, 1993; Burr et al., 2012). The association of dark dunes with the MFF on Mars, which is probably ignimbrite (e.g., Scott and Tanaka, 1982; Mandt et al., 2008, 2009), provides another fascinating association to consider. The high-altitude, ignimbrite-dominated, cold-desert environment of the Puna may indeed be a compelling analog for the MFF.

Finally, our evolutionary model for dynamic yet stable coarse megariipples in the Puna that grow through infiltration and accretion may be useful on Mars. Rovers on Mars have encountered powder-soft cores of granule ripples and

gravel/granule surface. Perhaps permeable gravels act as sand and silt traps on Mars, and undergo a growth similar to that of the Puna megariipples. Continued studies of the Puna megariipples will provide further insight on these enigmatic Mars landforms.

## CONCLUSIONS

Gravel megariipples in the Puna of Argentina may be the most extreme aeolian bedforms on Earth. Sedimentological and morphological analysis is supported by field, experimental, and numerical characterization of aeolian transport to reveal the conditions for formation and a model of their origin. The megariipples are coarse gravel-mantled bedforms with cores of sand and silt developed on eroded bedrock ignimbrite, aeolian erosion of which yields the bimodal association of dense volcanic and metamorphic clasts and lighter pumice clasts that makes up the gravels. Locally the gravels may be augmented by lithics from the surrounding basement.

Field, experimental, and theoretical characterization of wind characteristics and aeolian transport in the Puna demonstrate the role that saltating sand and pumice plays in inducing lithic clasts to creep. The intimate association of pumice and lithics in the bedforms reflects this, with strong evidence that bedforms form by organization of the lag gravel into stable bedforms by creep of gravel clasts induced by impact of saltating pumice. An undulating topography on the bedrock ignimbrite plays an important role in focusing bedform nucleation on upslopes and crests. The best-developed bedforms cap a topography with amplitudes as high as 2 m and wavelengths of 30 m or more, although the bedform itself makes up only ~30 cm of the topography. The strong role of bedrock topography in the location of the largest megariipples obviates a relationship between ripple wavelengths and particle trajectories. This complicates the classification of these features.

Once formed, bedforms are stable. Because the transport and deposition of sand and gravel is decoupled, the sand/silt cores of the gravel-mantled bedforms are interpreted to have been trapped by the gravels. Kinetic sieving of sand and silt through the gravel results in a gravel-mantled bedform as the gravel pavement is lifted up by the growing sandy core. This model for entrapment, infiltration, and growth implies that cores of the megariipples are accreted over time after a stable gravel accumulation has developed. A role for “shadowing” in the growth of the megariipples is also likely. These observations connote that the largest features are not ripples in the sense of migrating bedforms, but

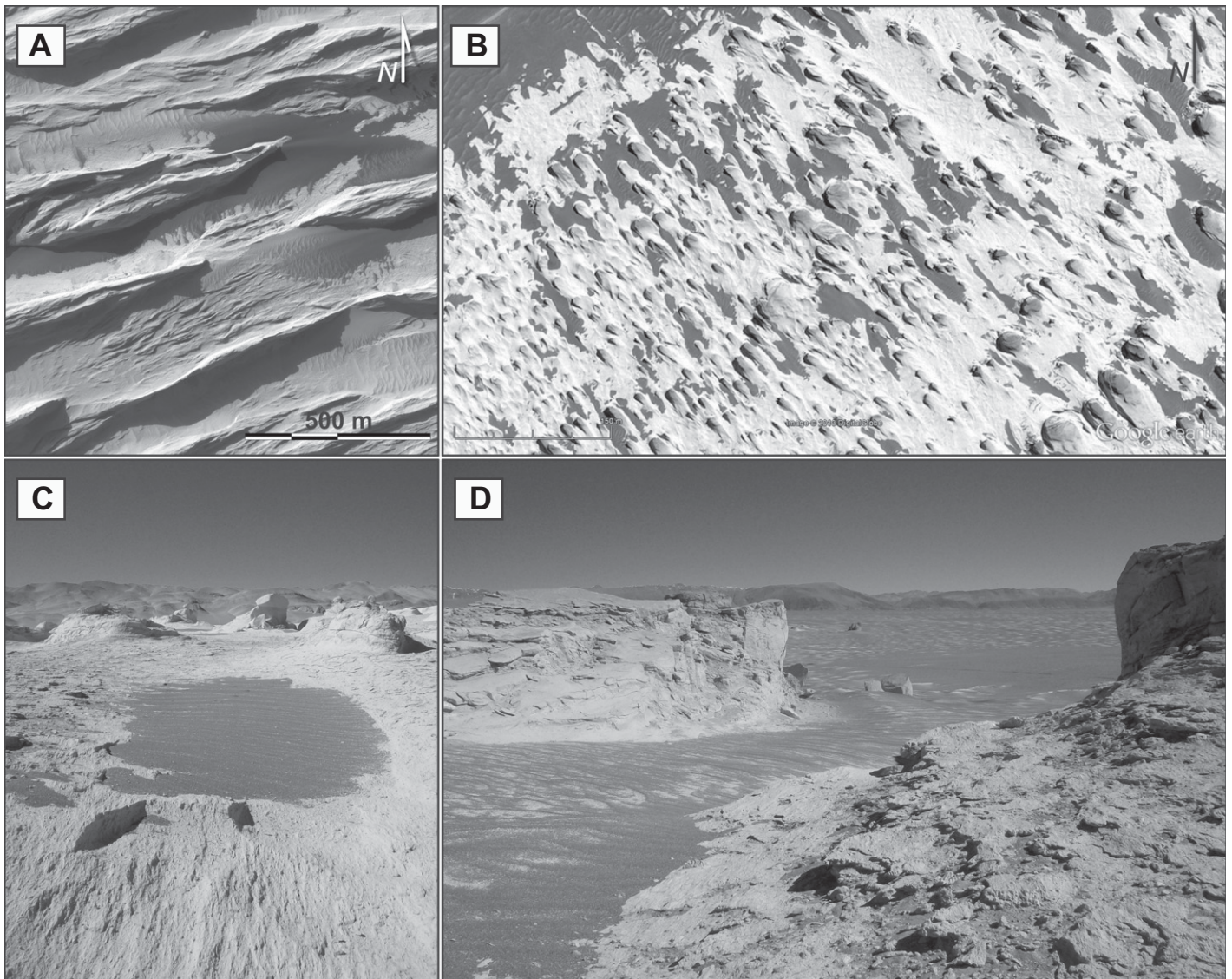


**Figure 12.** (A) Dark material forming bedforms in the swales and interfoils between yardangs in the Medusa Fossae Formation of Mars. (Extract from HiRISE image PSP\_008621\_1750.) Scale bar is 500 m. (B) Dark lag gravel forming bedforms in the swales or interfoils between yardangs in the Campo Piedra Pomez in the Argentinean Puna. (Extract from Geoeye image.) Scale bar is 100 m. (C and D) Field photos of part of the area shown in B showing details of the gravel bedforms and their relationship to the local topography.

rather nucleation sites of wind-transported sediment. The largest and most extensive bedforms may be stable “equilibrium” features that alter wind flow and saltation pathways to promote trough deepening, becoming more topographically extreme with time.

This region of the Puna represents a rare natural laboratory for the development of extreme aeolian sediments and bedforms. The association of a bedrock lithology (ignimbrite) that is susceptible to aeolian erosion, forms an undulating erosional topography, and is rich in a bimodal association of clasts with complementary aeolian behavior, in a region dominated by aeolian activity is, to our knowledge, unique on Earth.

The relevance to Mars extends beyond the fact that in size and aspect the Puna megaripples are essentially the same as small TARs on Mars. These aeolian gravel bedforms consist of materials that have similar equivalent weight ( $mg$ ) to those composing the granule ripples at Meridiani Planum, Mars, even though the ones on Mars probably took longer to form because of less-frequent threshold winds on the planet. Additionally, the spatial relationships among these Puna megaripples, topography, and bedrock are analogous to relationships among TARs, topography, and bedrock on Mars. Therefore, study of the Puna could help reconcile current models of TARs with the recognition that some PBRs

may be produced by aeolian erosion. Finally, our observation that the gravels that mantle the megaripples are locally derived has implications for the source material in martian ripples, dunes, and TARs. Such a local derivation would obviate the need for large-scale transport of sediment as has been inferred for dark dunes on Mars.

#### ACKNOWLEDGMENTS

We dedicate this work to the memory of our collaborator Ron Greeley. His support, encouragement, and wisdom was critical to implementing this work. This work is conducted under the auspices of NASA Mars Fundamental Research Program grant NNX10AP79G (Principal Investigator de Silva). Jose Viramonte’s knowledge, support, and enthusiasm were a major

boon for this work. Ralph Lorenz designed and loaned us the time-lapse cameras; his advice and keen insight are always appreciated. Agustin Ortiz is thanked for enthusiastic support in the field and discussions about gravel componentry. We are also indebted to the staff at the Arizona State University wind tunnel facility (supported in part by the NASA Planetary Geology and Geophysics program) for their support and advice during our experiments there. Devon Burr is thanked for extensive discussions about volcanoclastic sediment sources and dark dunes and strong interest in this work. Josh Emery and Devon Burr provided the IDL code used to compute saltation friction speed using the Greeley and Iversen (1985) method. Rob Sullivan and Mary Bourke are thanked for their advice on the wind tunnel experiments. The interest, insight, and comments of two anonymous reviewers and Associate Editor Nadine Barlow are deeply appreciated.

## REFERENCES CITED

- Ackert, R.P., Jr., 1989, The origin of isolated gravel ripples in the western Asgard Range, Antarctica: *Antarctic Journal of the United States*, v. 24, no. 5, p. 60–62.
- Anderson, R.S., 1987, A theoretical model for aeolian impact ripples: *Sedimentology*, v. 34, p. 943–956, doi:10.1111/j.1365-3091.1987.tb00814.x.
- Arnosio, M., Becchio, R., Viramonte, J., Gropelli, G., Norini, G., and Corazzato, C., 2005, Geología del complejo volcanico Cerro Blanco (26°45'S–67°45'O), Puna Austral: XVI Congreso Geológico Argentino, v. 1, p. 851–855.
- Bagnold, R.A., 1941, *The Physics of Blown Sand and Desert Dunes*: London, Chapman and Hall, 265 p.
- Balme, M.R., Berman, D.C., Bourke, M.C., and Zimbleman, J.R., 2008, Transverse Aeolian Ridges (TARs) on Mars: *Geomorphology*, v. 101, p. 703–720, doi:10.1016/j.geomorph.2008.03.011.
- Berman, D.C., Balme, M.R., Rafkin, S.C.R., and Zimbleman, J.R., 2011, Transverse Aeolian Ridges (TARs) on Mars II: Distributions, orientations, and ages: *Icarus*, v. 213, p. 116–130, doi:10.1016/j.icarus.2011.02.014.
- Bourke, M.C., Wilson, S.A., and Zimbleman, J.R., 2003, The variability of transverse Aeolian ridges in troughs on Mars, in *Proceedings, Lunar and Planetary Science Conference XXXIV*: Houston, Texas, Lunar and Planetary Institute, abstract 2090 (CD-ROM).
- Breed, C.S., and Grow, T., 1979, Morphology and distribution of dunes in sand seas observed by remote sensing, in *McKee, D.E., ed., A Study of Global Sand Seas*: U.S. Geological Survey Professional Paper 1052, p. 253–304.
- Burr, D.M., Zimbleman, J.R., de Silva, S.L., Bridges, N.T., Chojnacki, M., and Qualis, F.B., 2012, Testing the volcanoclastic hypothesis for martian dune sediments: The Medusae Fossae Formation, Mars, and Andean ignimbrites, Earth, in *Third International Planetary Dunes Workshop: Remote Sensing and Data Analysis of Planetary Dunes*: Houston, Texas, Lunar and Planetary Institute Contribution No. 1673, p. 17–18.
- Bridges, N.T., Bourke, M.C., Geissler, P.E., Banks, M.E., Colon, C., Diniega, S., Golombek, M.P., Hansen, C.J., Mattson, S., McEwen, A.S., Mellon, M.T., Stantzos, N., and Thomson, B.J., 2012, Planet-wide sand motion on Mars: *Geology*, v. 40, p. 31–34, doi:10.1130/G32373.1.
- Bridges, N.T., Geissler, P., Silvestro, S., and Banks, M., 2013, Bedform migration on Mars: Current results and future plans: *Aeolian Research*, v. 9, p. 133–151, doi:10.1016/j.aeolia.2013.02.004.
- Cas, R.A.F., and Wright, J.V., 1992, *Volcanic successions, Modern and Ancient: A Geological Approach to Processes, Products and Successions*: London, New York, Chapman Hall, 528 p.
- Delgado-Fernandez, I., Jackson, D.W.T., Cooper, J.A.G., Baas, A.C.W., Beyers, J.H.M., and Lynch, K., 2013, Field characterization of three-dimensional lee-side airflow patterns under offshore winds at a beach-dune system: *Journal of Geophysical Research: Earth Surface*, v. 118, p. 706–721, doi:10.1002/jgrf.20036.
- de Silva, S.L., 1989, Geochronology and stratigraphy of the ignimbrites from the 21°30'S to 23°30'S portion of the Central Andes of northern Chile: *Journal of Volcanology and Geothermal Research*, v. 37, p. 93–131, doi:10.1016/0377-0273(89)90065-6.
- de Silva, S., 2010, The largest wind ripples on Earth: Comment: *Geology*, v. 38, p. e218, doi:10.1130/G30780C.1.
- de Silva, S.L., and Bailey, J.E., 2011, The geomorphic expression and surface patterns of ash-flow deposits on Earth: Implications for the presence of ash deposits on Mars, in *Proceedings, American Geophysical Union, Fall Meeting 2011, Abstract V31A-2509*.
- de Silva, S.L., Bailey, J.E., Mandt, K.E., and Viramonte, J.M., 2010, Yardangs in terrestrial ignimbrites: Synergistic remote and field observations on Earth with applications to Mars: *Planetary and Space Science*, v. 58, p. 459–471, doi:10.1016/j.pss.2009.10.002.
- de Silva S.L., Burr, D.M., Ortiz, A., Spagnuolo, M., Zimbleman, J.R., and Bridges, N.T., 2012, Dark aeolian megaripples from the Puna of Argentina: Sedimentology and implications for dark dunes on Mars, in *Proceedings, Lunar and Planetary Science Conference XLIII*: Houston Texas, Lunar and Planetary Institute, abstract 2038.
- Edgett, K.S., and Lancaster, N., 1993, Volcanoclastic aeolian dunes: Terrestrial examples and application to martian sands: *Journal of Arid Environments*, v. 25, p. 271–297, doi:10.1006/jare.1993.1061.
- Gillies, J.A., Nickling, W.G., Tilson, M., and Furtak-Cole, E., 2012, Wind-formed gravel bed forms, Wright Valley, Antarctica: *Journal of Geophysical Research*, v. 117, F04017, doi:10.1029/2012JF002378.
- Greeley, R., and Iversen, J.D., 1985, *Wind as a Geological Process on Earth, Mars, Venus and Titan*: New York, Cambridge University Press, 333 p.
- Greeley, R., and Peterfreund, A.R., 1981, Aeolian “megaripples”: Examples from Mono Craters, California and North Iceland: *Geological Society of America Abstracts with Programs*, v. 13, no. 7, p. 463.
- Greeley, R., Lee, S., and Thomas, P., 1992, *Martian aeolian processes, sediments, and features*, in *Matthews, M.S., Kieffer, H.H., Jakosky, B.M., and Snyder, C.W., eds., Mars: Tucson, The University of Arizona Press, p. 730–766*.
- Haberle, R.M., Murphy, J.R., and Schaeffer, J., 2003, Orbital change experiments with a Mars general circulation model: *Icarus*, v. 161, p. 66–89, doi:10.1016/S0019-1035(02)00017-9.
- Hepper, E.N., Buschiazzo, D.E., Hevia, G.G., Urioste, A., and Anton, L., 2006, Clay mineralogy, cation exchange capacity and specific surface area of loess soils with different volcanic ash contents: *Geoderma*, v. 135, p. 216–223, doi:10.1016/j.geoderma.2005.12.005.
- Izenberg, O., Yizhaq, H., Tsoar, H., Wenkart, R., Karnieli, A., Kok, J.F., and Katra, I., 2011, Megaripple flattening due to strong winds: *Geomorphology*, v. 131, p. 69–84, doi:10.1016/j.geomorph.2011.04.028.
- Jackson, D., Beyers, M., Lynch, K., Cooper, A., Baas, A., and Delgado-Fernandez, I., 2011, Investigation of three-dimensional wind flow behaviour over coastal dune morphology under offshore winds using Computational Fluid Dynamics (CFD) and ultrasonic anemometry: *Earth Surface Processes and Landforms*, v. 36, p. 1113–1124, doi:10.1002/esp.2139.
- Jackson, D.W.T., Beyers, M., Delgado-Fernandez, I., Baas, A.C.W., Cooper, J.A.G., and Lynch, K., 2013, Airflow reversal and alternating corkscrew vortices in foredune wake zones during perpendicular and oblique offshore winds: *Geomorphology*, v. 187, p. 86–93, doi:10.1016/j.geomorph.2012.12.037.
- Jerolmack, D.J., Mohrig, D., Grotzinger, J.P., Fike, D., and Watters, W.A., 2006, Spatial grain size sorting in aeolian ripples and estimation of wind conditions on planetary surfaces: Application to Meridiani Planum, Mars: *Journal of Geophysical Research*, v. 111, E12S02, doi:10.1029/2005JE002544.
- Kok, J.F., Parteli, E.J.R., Michaels, T.I., and Bou Karam, D., 2012, The physics of wind-blown sand and dust: *Reports on Progress in Physics*, v. 75, 106901, doi:10.1088/0034-4885/75/10/106901.
- Krumbein, W.C. and Aberdeen, E., 1937, The sediments of Barataria Bay: *Journal of Sedimentary Petrology*, v. 7, no. 1, p. 3–17.
- Malin, M.C., and Edgett, K.E., 2001, Mars Global Surveyor Mars Orbiter Camera: Interplanetary cruise through primary mission: *Journal of Geophysical Research*, v. 106, p. 23,429–23,570, doi:10.1029/2000JE001455.
- Mandt, K., de Silva, S.L., Zimbleman, J.R., and Crown, D.A., 2008, The origin of the Medusae Fossae Formation, Mars: Insights from a synoptic approach: *Journal of Geophysical Research*, v. 113, E12011, doi:10.1029/2008JE003076.
- Mandt, K., de Silva, S., Zimbleman, J., and Wyrick, D., 2009, Distinct erosional progressions in the Medusae Fossae Formation, Mars, indicate contrasting environmental conditions: *Icarus*, v. 204, p. 471–477, doi:10.1016/j.icarus.2009.06.031.
- McEwen, A.S., Eliason, E.M., Bergstrom, J.W., Bridges, N.T., Hansen, C.J., Delamere, W.A., Grant, J.A., Gulick, V.C., Herkenhoff, K.E., Keszthelyi, L., Kirk, R.L., Mellon, M.T., Squyres, S.W., Thomas, N., and Weitz, C.M., 2007, Mars Reconnaissance Orbiter's High Resolution Imaging Science Experiment (HiRISE): *Journal of Geophysical Research*, v. 112, E05S02, doi:10.1029/2005JE002605.
- Milana, J.P., 2009, Largest wind ripples on Earth?: *Geology*, v. 37, p. 343–346, doi:10.1130/G25382A.1.
- Milana, J.P., Forman, S., and Krohling, D., 2010, The largest wind ripples on earth: Reply: *Geology*, v. 38, p. e219–e220, doi:10.1130/G31354Y.1.
- Montgomery, D.R., Bandfield, J.L., and Becker, S.K., 2012, Periodic bedrock ridges on Mars: *Journal of Geophysical Research*, v. 117, E03005, doi:10.1029/2011JE003970.
- Ortiz, A., 2011, Estudio de unidades piroclásticas a partir del análisis petrográfico de fragmentos líticos: Complejo Volcanico Cerro Blanco, Puna Austral: Tesis Profesional, Facultad de Ciencias Naturales, Escuela de Geología, Universidad de Salta, Argentina, 70 p.
- Scott, D.H., and Tanaka, K.L., 1982, Ignimbrites of Amazonis Planitia region of Mars: *Journal of Geophysical Research*, v. 87, p. 1179–1190, doi:10.1029/JB087iB02p01179.
- Selby, M.J., Rains, B.B., and Palmer, R.W.P., 1974, Eolian deposits of the ice-free Victoria Valley, Southern Victoria Land, Antarctica: *New Zealand Journal of Geology and Geophysics*, v. 17, p. 543–562, doi:10.1080/00288306.1973.10421580.
- Shao, Y.P., and Lu, H., 2000, A simple expression for wind erosion threshold friction velocity: *Journal of Geophysical Research*, v. 105, p. 22,437–22,443, doi:10.1029/2000JD900304.
- Sharp, R.P., 1963, Wind ripples: *Journal of Geology*, v. 71, p. 617–636.
- Shockey, K.M., and Zimbleman, J.R., 2013, Analysis of transverse aeolian ridge profiles derived from HiRISE images of Mars: *Earth Surface Processes and Landforms*, v. 38, p. 179–182, doi:10.1002/esp.3316.
- Silvestro, S., Fenton, L.K., Vaz, D.A., Bridges, N.T., and Ori, G.G., 2010, Ripple migration and dune activity on Mars: Evidence for dynamic wind processes: *Geophysical Research Letters*, v. 37, L20203, doi:10.1029/2010GL044743.
- Smyth, T.A.G., Jackson, D.W.T., and Cooper, J.A.G., 2013, Three dimensional airflow patterns within a coastal trough-bowl blowout during fresh breeze to hurricane force winds: *Aeolian Research*, v. 9, p. 111–123, doi:10.1016/j.aeolia.2013.03.002.
- Soderblom, L.A., and 44 others, 2004, Soils at Eagle Crater and Meridiani Planum at the Opportunity Rover landing site: *Science*, v. 306, p. 1723–1726, doi:10.1126/science.1105127.
- Strecker, M.R., Alonso, R.N., Bookhagen, B., Carrapa, B., Hilley, G.E., Sobel, E.R., and Trauth, M.H., 2007, Tectonics and climate of the southern central Andes: *Annual Review of Earth and Planetary Sciences*, v. 35, p. 747–787, doi:10.1146/annurev.earth.35.031306.140158.
- Sullivan, R., Banfield, D., Bell, J.F., III, Calvin, W., Fike, D., Golombek, M., Greeley, R., Grotzinger, J., Herkenhoff, K., Jerolmack, D., Malin, M., Ming, D., Soderblom, L.A., Squyres, S.W., Thompson, S., Watters, W.A., Weitz, C.M., and Yen, A., 2005, Aeolian processes at the Mars Exploration Rover Meridiani Planum landing site: *Nature*, v. 436, p. 58–61, doi:10.1038/nature03641.

- Sullivan, R., Arvidson, R., Grotzinger, J., Knoll, A., Golombek, M., Jolliff, B., Squyres, S., and Weitz, C., 2007, Aeolian geomorphology with MER OPPORTUNITY at Meridiani Planum, Mars, *in* Proceedings, Lunar and Planetary Science Conference XXXVIII: Houston, Texas, Lunar and Planetary Institute, abstract 2048.
- Teruggi, M., 1957, The nature and origin of Argentine loess: *Journal of Sedimentary Research*, v. 27, p. 322–332.
- Ward, A.W., 1979, Yardangs on Mars: Evidence of recent wind erosion: *Journal of Geophysical Research*, v. 84, p. 8147–8166, doi:10.1029/JB084iB14p08147.
- Wells, S.G., Dohrenwend, J.C., McFadden, L.D., Turrin, B.D., and Mahrer, K.D., 1985, Late Cenozoic landscape evolution on lava flow surfaces of the Cima volcanic field, Mojave Desert, California: *Geological Society of America Bulletin*, v. 96, p. 1518–1529, doi:10.1130/0016-7606(1985)96<1518:LCLEOL>2.0.CO;2.
- Wilson, S.A., and Zimbelman, J.R., 2004, The latitude-dependent nature and physical characteristics of transverse aeolian ridges on Mars: *Journal of Geophysical Research*, v. 109, E10003, doi:10.1029/2004JE002247.
- Yizhaq, H., Isenberg, O., Wenkart, R., Tsoar, H., and Karnieli, A., 2009, Morphology and dynamics of aeolian megaripples in Nahal Kasuy, southern Israel: *Israel Journal of Earth Sciences*, v. 57, p. 149–165, doi:10.1560/IJES.57.3-4.149.
- Yizhaq, H., Katra, I., Isenberg, O., and Tsoar, H., 2012, Evolution of megaripples from a flat bed: *Aeolian Research*, v. 6, p. 1–12, doi:10.1016/j.aeolia.2012.05.001.
- Zimbelman, J.R., 2008 Transverse aeolian ridges on Mars: Results obtained from analysis of HiRISE images, *in* Planetary Dunes Workshop: A Record of climate Change: Lunar and Planetary Institute Contribution No. 1403, p. 83–84.
- Zimbelman, J.R., 2010, Transverse Aeolian Ridges on Mars: First results from HiRISE images: *Geomorphology*, v. 121, p. 22–29, doi:10.1016/j.geomorph.2009.05.012.
- Zimbelman, J.R., Williams, S.H., and Johnston, A.K., 2012, Cross-sectional profiles of sand ripples and dunes: a method for discriminating between formational mechanisms: *Earth Surface Processes and Landforms*, v. 37, p. 1120–1125.

SCIENCE EDITOR: CHRISTIAN KOEBERL  
ASSOCIATE EDITOR: NADINE BARLOW

MANUSCRIPT RECEIVED 6 MAY 2013  
REVISED MANUSCRIPT RECEIVED 5 SEPTEMBER 2013  
MANUSCRIPT ACCEPTED 3 OCTOBER 2013

Printed in the USA